Materials and Structures (2025) 58:182
https://doi.org/10.1617/s11527-025-02687-w

RILEM TC REPORT

Mechanical properties of 3D printed concrete: a RILEM TC 304-ADC interlaboratory study — flexural and tensile strength

Rob Wolfs · Jelle Versteege · Manu Santhanam · Shantanu Bhattacherjee · Freek Bos · Annika Robens-Radermacher · Shravan Muthukrishnan · Costantino Menna · Onur Ozturk · Nilufer Ozyurt · Josef Roupec · Christiane Richter · Jörg Jungwirth · Luiza Miranda · Rebecca Ammann · Jean-François Caron · Victor de Bono · Renate Monte · Iván Navarrete · Claudia Eugenin · Hélène Lombois-Burger · Bilal Baz · Maris Sinka · Alise Sapata · Ilhame Harbouz · Yamei Zhang · Zijian Jia · Jacques Kruger · Jean-Pierre Mostert · Katarina Šter · Aljoša Šajna · Abdelhak Kaci · Said Rahal · Chalermwut Snguanyat · Arun Arunothayan · Zengfeng Zhao · Inka Mai · Inken Jette Rasehorn · David Böhler · Niklas Freund · Dirk Lowke · Tobias Neef · Markus Taubert · Daniel Auer · C. Maximilian Hechtl · Maximilian Dahlenburg · Laura Esposito · Richard Buswell · John Kolawole · Muhammad Nura Isa · Xingzi Liu · Zhendi Wang · Kolluru Subramaniam · Viktor Mechtcherine

Received: 28 November 2024 / Accepted: 12 May 2025 / Published online: 24 June 2025

Abstract This paper discusses the flexural and tensile strength properties of 3D printed concrete, based on the results of a RILEM TC 304-ADC interlaboratory study on mechanical properties. These properties are determined using different testing techniques, including 3- and 4-point flexural tests, splitting tests, and uniaxial tension tests, on specimens extracted from large 3D printed elements in accordance with

This paper has been prepared by representatives of participating laboratories and a writing group within the framework of RILEM TC 304-ADC 'Assessment of Additively Manufactured Concrete Materials and Structures' and further reviewed and approved by all members of the RILEM TC 304-ADC.

TC Chair: Viktor Mechtcherine.
TC Deputy chair: Freek Bos.
TC Members:
Rebecca Ammann, Arun Arunothayan, Daniel Auer, Bilal Baz, Shantanu Bhattacherjee, David Böhler, Richard Buswell, Laura Caneda Martinez, Jean-François Caron, Yu Chen, Maximilian Dahlenburg, Victor de Bono, Geert De Schutter, Laura Esposito, Claudia Eugenin, Liberato Ferrara, Niklas Freund, Lukas Gebhard, Lucija Hanžič, Ilhame Harbouz, C. Maximilian Hechtl, Muhammad Nura Isa, Egor Ivaniuk, Smrati Jain, Zijian Jia, Zhengwu Jiang, Jörg Jungwirth, Abdelhak Kaci, Emmanuel Keita, John Kolawole, Jacques Kruger, Cezary Kujath, Lucas Lima, Xingzi Liu, Hélène Lombois-Burger, Dirk Lowke, Inka Mai, Costantino Menna, Luiza Miranda, Renate Monte, Sandro Moro, Jean-Pierre Mostert, Shravan Muthukrishnan, Iván Navarrete, Tobias Neef, Behzad Nematollahi, Onur Ozturk, Nilufer Ozyurt, Said Rahal, Inken Jette Rasehorn, Atta Ur Rehman, Christiane Richter, Annika Robens-Radermacher, Josef Roupec, Nicolas Roussel, Aljoša Šajna, Manu Santhanam, Alise Sapata, Maris Sinka, Chalermwut Snguanyat, Mateja Štefančič, Katarina Šter, Kolluru Subramaniam, Markus Taubert, Jörg F. Unger, Jolien Van Der Putten, Kim Van Tittelboom, Gideon van Zijl, Jelle Versteege, Zhendi Wang, Timothy Wangler, Daniel Weger, Rob Wolfs, Yamei Zhang, Yi Zhang, Zengfeng Zhao.

R. Wolfs · J. Versteege
Eindhoven University of Technology, Eindhoven, The Netherlands

M. Santhanam
Indian Institute of Technology Madras, Chennai, India

S. Bhattacherjee
Tvasta, Chennai, India

a prescribed study plan. The relationship between compressive and flexural or tensile strengths, cast or printed samples, different types of tests, and different loading orientations, are analysed to understand the influence of 3D printing. As expected, the strength can reduce significantly when the main tensile stress is acting perpendicular to the interface between layers. The role of deviations from the standard study procedure, in terms of the time interval between the placing of subsequent layers, or the adoption of a different curing strategy, are also assessed. While the increased time interval significantly impacts the strength in the critical direction, the use of variable curing conditions does not seem to have a clear-cut effect on the strength ratios of the printed to cast specimens. Additionally, the paper looks at the variability in the results for the printed specimens, in order to emphasize the need for multiple replicates for obtaining a proper result. An extensive insight into the aspects affecting the variability is presented in the paper. Finally, with the limited dataset available for specimens tested at a larger scale, it is difficult to

F. Bos (✉) · D. Auer · C. M. Hechtl · M. Dahlenburg
Technical University of Munich, Munich, Germany
e-mail: freek.bos@tum.de

A. Robens-Radermacher
Bundesanstalt Für Materialforschung Und -Prüfung, Berlin, Germany

S. Muthukrishnan · T. Neef · M. Taubert · V. Mechtcherine
TU Dresden, Dresden, Germany

S. Muthukrishnan · A. Arunothayan
Swinburne University of Technology, Melbourne, Australia

C. Menna
University of Naples Federico II, Naples, Italy

O. Ozturk · N. Ozyurt
Bogazici University, Istanbul, Turkey

J. Roupec
Brno University of Technology, Brno, Czech Republic

C. Richter · J. Jungwirth
Munich University of Applied Sciences, Munich, Germany

L. Miranda
Ghent University, Ghent, Belgium

R. Ammann
ETH Zurich, Zurich, Switzerland

J.-F. Caron · V. de Bono
Ecole Des Ponts ParisTech, Champs-Sur-Marne, France

R. Monte
University of São Paulo, São Paulo, Brazil

I. Navarrete · C. Eugenin
Pontificia Universidad Catolica de Chile, Santiago, Chile

H. Lombois-Burger · B. Baz
Holcim Innovation Center, Saint-Quentin-Fallavier, France

M. Sinka · A. Sapata
Riga Technical University, Riga, Latvia

I. Harbouz
Université de Sherbrooke, Sherbrooke, Canada

Y. Zhang · Z. Jia
Southeast University, Nanjing, China

J. Kruger · J.-P. Mostert
Stellenbosch University, Stellenbosch, South Africa

K. Šter · A. Šajna
ZAG - Slovenian National Building and Civil Engineering Institute, Ljubljana, Slovenia

A. Kaci · S. Rahal
CY Cergy Paris Université, Cergy, France

C. Snguanyat
SCG Cement-Building Materials, Bangkok, Thailand

Z. Zhao
Tongji University, Shanghai, China

I. Mai · I. J. Rasehorn
Technical University of Berlin, Berlin, Germany

D. Böhler · N. Freund · D. Lowke
Technical University of Braunschweig, Brunswick, Germany

L. Esposito
Heidelberg Materials, Heidelberg, Germany

R. Buswell · J. Kolawole · M. N. Isa · X. Liu
Loughborough University, Loughborough, UK

Z. Wang
China Building Materials Academy, Beijing, China

K. Subramaniam
Indian Institute of Technology Hyderabad, Kandi, India

arrive at a clear understanding of the role of specimen size (i.e., greater number of layers).

Keywords 3D concrete printing · Digital fabrication · Flexural strength · Tensile strength · Interlayer bond strength

1 Introduction

Extrusion-based 3D concrete printing (3DCP) has gained considerable attention in recent years in both academia and industry [1–3]. Following the typical development curve of an emerging technology, industry activities are gradually shifting from demonstration projects and proof-of-concepts, to real-life structural applications of printed concrete [4, 5]. To support this transition, understanding the mechanical properties of printed concrete is key, to realize structurally safe and durable applications, and prove compliance to building codes. This is, however, not straightforward as 3D printed concrete differs from conventional construction practices (casting in formwork) due to the nature of the additive manufacturing process. No formwork is present to support the fresh material during printing, or to subsequently protect the surfaces of the printed structures. Inevitably, printed structures are composed out of multiple layers, which introduces numerous interfaces (or interlayers) into the final objects. These objects are typically geometrically more intricate than their conventionally produced counterparts, e.g., thinner, hollow, or curved. Finally, the majority of printable cementitious materials contain relatively high cement contents and are limited in maximum aggregate size [6–8]. The combined effect of these features requires to revisit existing testing protocols and well established (design) rules for concrete in the light of 3DCP. In the meantime, the majority of applications remain of a non-structural nature (e.g. lost formwork applications), or large-scale experimental programs have to be performed to demonstrate compliance by means of destructive testing [9–11].

To gain insight into the mechanical properties of 3D printed concrete, and stimulate the development towards common testing procedures, the RILEM Technical Committee (TC) 304-ADC has initiated an interlaboratory study on the mechanical properties of 3D printed concrete (ILS-mech). In total, 30 participating laboratories, spread across the globe, performed an experimental program in 2023, based on a detailed study plan prepared by TC members [12]. This resulted in approximately 5000 data points on the compressive strength, flexural and tensile strength, and E-modulus of printable concrete. The study plan provided guidelines on specimen preparation and testing procedure, but each participating laboratory could select their own material composition and printing process settings, which were reported together with the test results in preprepared spreadsheet templates. An overview of the participants, the adopted parameters, and main results, is provided in [13], while the final dataset is publicly accessible [14] and elaborated on in an accompanying contribution [15]. Based on the ILS-mech results, two in-depth analyses have been conducted. The first targets the compressive strength and E-modulus properties of printable concrete [16]. The second, which is the topic of this contribution, targets the flexural and tensile strength properties of 3D printed concrete.

Various experimental results of the flexural and tensile properties of printed concrete have already been presented, see e.g. [17–20], but typically concern isolated studies based on a single material composition and printing process. As a result, the reported effects of relevant parameters (e.g. the layer vs. loading orientation, or the effect of an increased time interval between layers), can vary significantly and in some cases even contradict each other. Based on the extensive dataset collected in the ILS-mech, this contribution aims to perform analyses of results spanning across a representative range of printable materials and 3D printing systems, and provide generalizable conclusions which may form a basis for test recommendations and future standards.

Firstly, the typical material compositions and specimen preparation will be discussed, along with an overview of the test methods considered in this contribution: 3-Point and 4-Point bending tests, splitting tests, and uniaxial tensile tests (Sect. 2). Then, an overview of the strength values obtained across all participants of the ILS-mech will be provided, along with some first observations (Sect. 3). In Sect. 4, the main analyses of flexural and tensile strength properties will take place. Here, a distinction will be made between the influence of test type on these strength values (Sect. 4.2), the influence of loading and specimen orientation (Sect. 4.3), and the

influence of specimen size (Sect. 4.4) and specimen location (Sect. 4.5). Then, the density values will be discussed (Sect. 4.6), followed by strength values obtained on specimens produced with a deviation from default settings: increased time interval between the layers (Sect. 4.7) and a variation in curing conditions (Sect. 4.8). Finally, a discussion on variability (Sect. 4.9) and outliers (Sect. 4.10) is provided. This contribution concludes in Sect. 5 with a summary of the main findings of the analyses on the ILS-mech results.

2 Materials and methods

The full details of the study plan, including the preparation of specimens and detailed methodologies for different types of tests conducted, are available in [12]. A gist of the overall plan that is relevant to the flexural and tensile strength properties is provided in this section and summarized in Table 1—all data of individual participating laboratories is moreover available in the ILS-mech database [14] and reviewed in [13].

2.1 Mix design and specimen preparation

Each participating laboratory could produce specimens using their own 3D printer system and mix design, since a distribution of a standardized mix was deemed impractical due to the strong interdependence between material and 3D printer system. Consequently, the participating laboratories used a variety of cementitious materials, including different types of binders, different sizes and gradations of fine aggregate, different combinations of chemical admixtures (superplasticizer (SP), viscosity modifying agent (VMA), accelerator (ACC) etc.), as well as different methods of delivery to the nozzle, in terms of using 1-component (‘1 K’) or 2-component (‘2 K’) systems. While it is impossible or perhaps even impractical to showcase each of these materials individually, the purpose of the ILS-mech was not to compare different types of mixture designs but rather to understand the interrelationships between different types of mechanical properties.

Specimens were prepared by means of 3D printing, where, much similar to the material compositions, a wide variety of printing settings (extrusion rate, nozzle velocity, nozzle dimensions, etc.) has been adopted among participating laboratories. For reference, cast samples have also been produced. After printing, an initial curing took place for 24–48 h, which typically consisted of covering the objects by plastic foil, after which they were stored in water until they had reached the minimum age for testing. The exact specimen age at which the tests were performed, varied between laboratories. For the purpose of assessment in this paper, however, only results ≥ 21 days of age are considered, and in cases where two strength values are compared, their respective age difference should be $\leq 11\%$ of the younger of the 2 ages.

Specimens were extracted from printed components by sawing, in the case of prismatic shapes (e.g., flexural tests), or by core-drilling for cylindrical specimens (e.g., splitting tests). In this extraction procedure, special attention was paid to recording the original layer orientations, as the influence of this orientation with respect to the direction of the load in the various tensile test considered, was also captured in the study, as illustrated in Table 1.

Another feature of the tests conducted in this study was the use of different scales, namely the ‘mortar’ scale and the ‘concrete’ scale, which was done in order to understand the role of multiple interlayers—both in the vertical direction and the horizontal direction—when larger scale systems are tested (the filament size is the same, hence the number of layers is more in a concrete system as compared to mortar). Note that this distinction only refers to the scale of the specimens, not to the material of which they are made—both mortar and concrete scale specimens produced by an individual laboratory were produced from the same material.

In addition to the prescribed ‘default’ printing and curing conditions, participants were invited to perform tests on ‘deviating’ specimens to assess the influence on the flexural and tensile strength: either by increasing the time interval between two layers during printing (designated as ‘Dev1’), or by applying a variation in curing conditions (designated as ‘Dev2’).

2.2 Experimental program

For the derivation of flexural and tensile strength properties, four different types of tests were

Table 1 Overview of experimental variables and values

Variable	Value
Material characteristic to be obtained	Uniaxial compressive strength [UCT] (Cast only) 3-Point and 4-Point Flexural strength [F3P & F4P] (Cast & Printed) Splitting tensile strength [STT] (Cast & Printed) Uniaxial tensile strength [UTT] (Cast & Printed)
Scale	Mortar (left): 40 × 40 × 160, or 50 × 50 × 200 mm or 50 dia × 150 height cylinders for flexure and tension, 40 mm cube or 50 mm dia and height cylinders for splitting Concrete (right): 100 × 100 × 400, or 100 × 100 × 500 mm or 150 dia × 300 mm height cylinders for flexure and tension, 150 mm cube or 150 mm dia and height cylinders for splitting 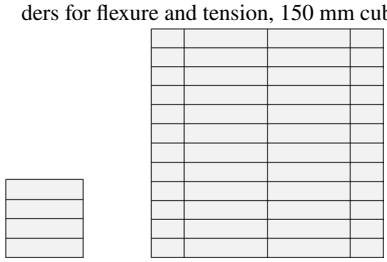
Specimen and load orientation	Depending on the specific test: for each test, 'mandatory' orientations were requested, and additional optional orientations were possible. The schematic below show illustrative cases for 'mortar' scale, all orientations are illustrated in [12] F3P and F4P: U.W, V.U, and W.U STT: W/U, V/W, and U/V (cubic) or W.U/V, V.U/W, and U.W/V (cylindrical) UTT: U and W 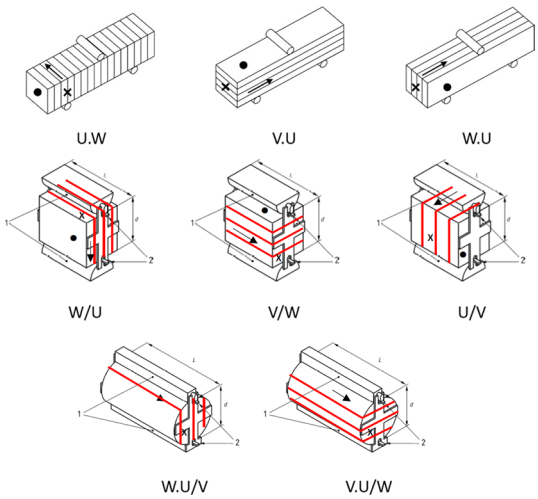
Mode of extraction	Sawing (prismatic specimens) Core-drilling (cylindrical specimens)
Process parameter	Default (continuous printing and standard curing conditions) Dev1 (increased time interval between layers) Dev2 (variation of curing conditions after printing)
Material age	Age at testing ≥ 21 days Age difference between testing of reference sample and printed samples should be ≤ 11% of the younger of the 2 ages
Material type	Plain concrete / mortar only (no (fibre) reinforcement)

performed: 3-Point and 4-Point bending tests (F3P and F4P), splitting tensile tests (STT), and uniaxial tensile tests (UTT). In all cases, the testing procedures as described in [12] were similar to those prescribed for conventional concrete or mortar testing in the affiliated EN standards, with the exception of adjustments to accommodate for differences in specimen size or preparation coming from the 3D printing process. For each test type and loading orientation considered, at least 5 valid data points should be submitted by all participants. The splitting tensile tests performed on cubic specimens constitutes the exception, where 9 data points were requested, spready evenly over specimens taken from three different locations over the printed object height (3 from the bottom, 3 from the middle, and 3 from the top part).

Before testing, specimen dimensions and weight were to be recorded, to compute density values. During the test, the failure force was to be recorded, which was then translated to a strength value as prescribed in the study plan [12]. Note that the conversion formula differs between the four test types and takes into account the different specimen dimensions and loading configuration.

3 Test results

This section provides an overview of the various flexural and tensile test results which fit within the scope of this contribution, as summarized in Table 1. These results are presented as absolute values for each individual lab-material combination. Figures 1, 2, 3 and 4 show the results for mortar scale specimens loaded in 3-point bending tests, as an illustrative example. The remainder of the results for 'default' process settings is visualized in the appendix (Figs. 13–25). While each figure represents a unique test type, loading orientation, and/or specimen size ('mortar' or 'concrete' scale), their layout is identical and composed as follows. The main graph in each figure shows the individual strength results in a box and whisker plot format, which provides a first visualization of the average values and variation within each series. Here, a 'series' refers to one set of datapoints provided by an individual lab-material combination: e.g., strength values derived by 3-point bending tests, performed on cast samples of mortar scale, executed by lab 01. Individual data points within one series are excluded from any further analysis, when their value exceeds two times the standard deviation of that series. These points are indicated as red dots in the box and whisker plot. The horizontal continuous line and dashed lines represent the average strength value and two times its standard deviation, respectively, computed based on the valid results of all labs for each particular test type. For the case of splitting tensile tests, both cubic and cylindrical specimens have been tested. The first is indicated by a blue colour, whereas the latter

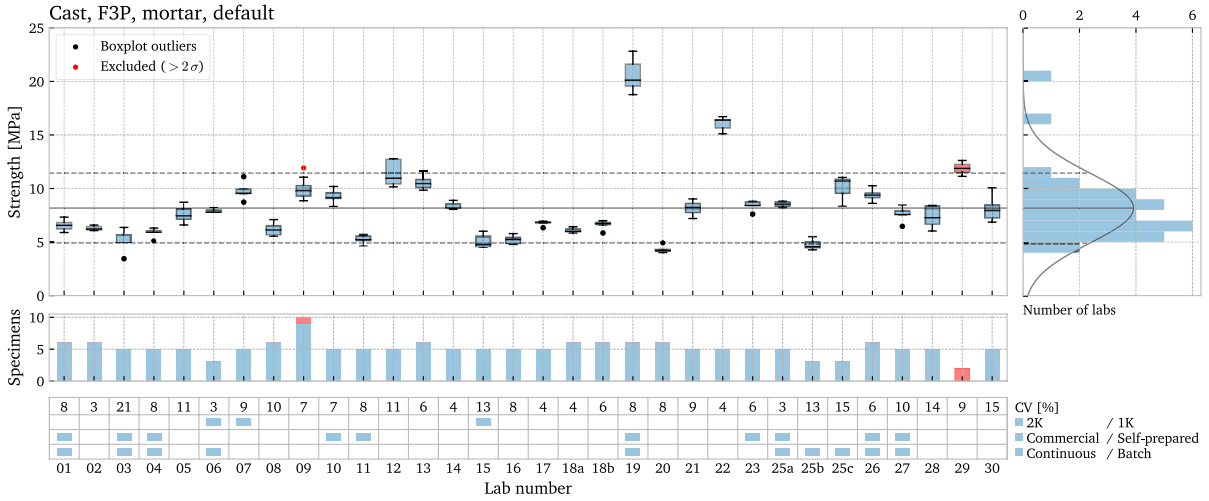

Fig. 1 Flexural strength values obtained by 3-Point bending tests performed on cast specimens of 'mortar' scale

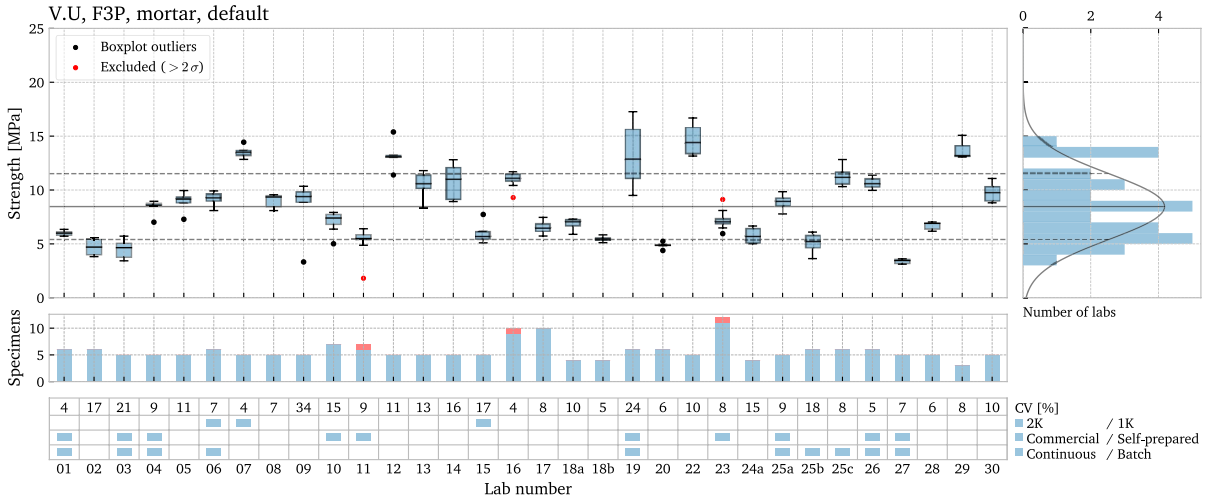

Fig. 2 Flexural strength values obtained by 3-Point bending tests performed on default printed specimens of 'mortar' scale, loaded in V.U orientation

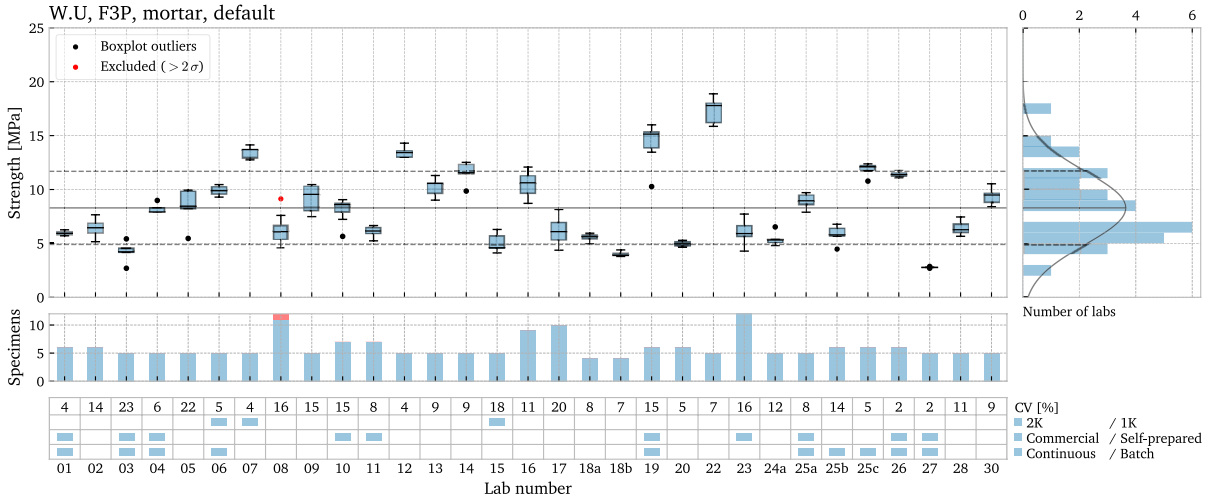

Fig. 3 Flexural strength values obtained by 3-Point bending tests performed on default printed specimens of 'mortar' scale, loaded in W.U orientation

is highlighted purple in the associated graphs in the appendix.

To the right of the box and whisker plot, a bar plot visualises the distribution of the average strength values across all labs. The black continuous line represents a normal distribution, as a reference.

Finally, below the box and whisker plot, information about each individual lab is provided. Firstly, the number of specimens n of each lab is visualized with a bar plot. Blue parts of the bar represent all valid data points, whereas red parts indicate excluded data. Note that series where the number of data points $n < 3$ are excluded from further analysis, as the amount of data points is deemed insufficient. These series are also indicated in red, see for instance lab29 in Fig. 1. Directly beneath, the coefficient of variation (CV) is given for each series, as a percentage value. Subsequently, printing material and system information is

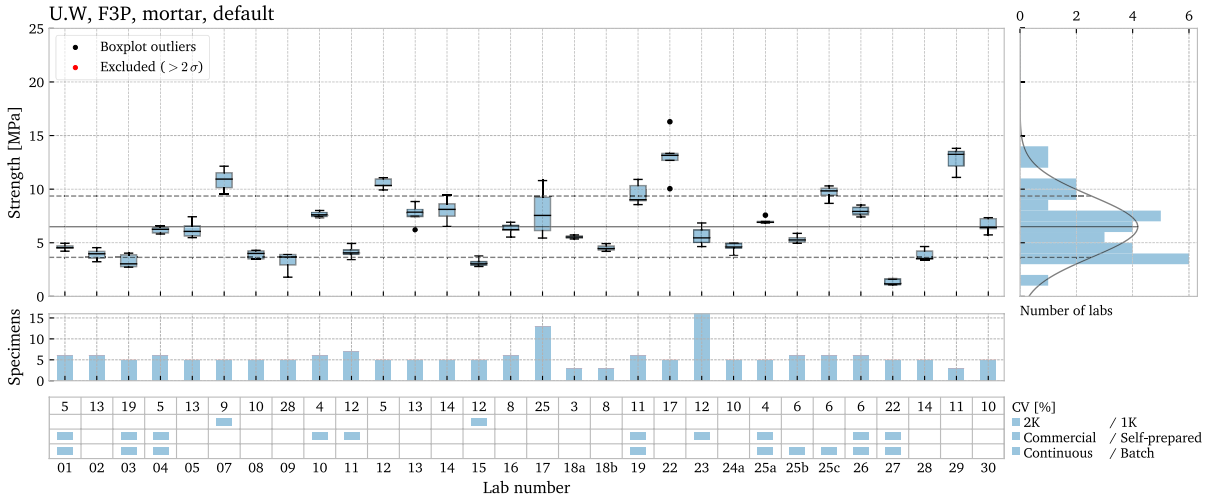

Fig. 4 Flexural strength values obtained by 3-Point bending tests performed on default printed specimens of 'mortar' scale, loaded in U.W orientation

listed, where a distinction is made between '1 K' or '2 K' mixtures, 'commercial' or 'self-prepared' mixtures, and 'continuous' or 'batch' mixing processes, based on the information provided by each lab [13], and finally the lab number itself. For instance, as seen in Fig. 1, lab 01 deployed a 1 K commercial mixture in a continuous mixing process and provided 6 data points of flexural strength values obtained by F3P on cast specimens of 'mortar' size. The corresponding coefficient of variation is 8%. Note that some labs have provided results using multiple printable mixtures, which are considered here as unique lab-material combinations and thus as individual series, see e.g., Lab 18a and 18b.

For each individual test type, the average strength values and their standard deviation, the average coefficients of variation and their standard deviation, and the corresponding number of labs which have performed the test, are compiled in Table 2 for the default process settings. Similar to the graph visualization, a distinction is made between printing and casting, loading orientation, as well as mortar and concrete scale specimens. At this stage, no distinction is made between choices in printing materials (e.g. '1 K' or '2 K' and 'commercial' or 'self-prepared' mixtures) and systems ('continuous' or 'batch' mixing) or specimen shape ('cubes' or 'cylinders' for splitting tensile tests) for the computation of these values. Note that the average values of the compressive strength obtained on cast samples is provided as a reference. For a detailed analysis of the compressive test results of the Interlaboratory Study, reference is made to [16].

For the tests performed on samples which have deviated from default process settings (Dev1: increased time interval and Dev2: variation in curing conditions), the results are reported for each individual lab-material combination. Since the adopted deviations vary significantly between labs, any averaging across labs such as done for default process settings (Table 2) does not hold. The results are listed in Tables 3, 4 and 5, along with the adopted Dev1 and Dev2 parameters. In Table 3, the average flexural strength ratio is reported, which is the ratio between the average strength for the printed specimens prepared with 'Dev1' settings to the Default cast specimens, obtained by 3-point bending tests. In the case of Table 4, the average flexural strength ratio is the ratio of the printed 'Dev2' specimens to the Default printed specimens, and the corresponding curing conditions are reported in Table 5. For both Dev1 and Dev2 results, only the F3P specimens have been listed. This is where the vast majority of data points is available, and consequently where the analyses in the following sections will focus on. For the remainder of results obtained by other tests (e.g., F4P or STT), reference is made to the ILS-mech database.

Finally, the density values as observed in cast and printed specimens are reported in Table 6, for 'mortar' and 'concrete' scale specimens. Here, the values

Table 2 Presentation of the full set of results for default process settings

Test type	Preparation	Scale	Orientation	μ Strength [MPa]	σ Strength [MPa]	μ CV [-]	σ CV [-]	n Labs
Compression test	Cast	Mortar		58.28	22.57	0.059	0.035	29
	Cast	Concrete		51.72	8.22	0.053	0.044	6
3-Point bending test	Cast	Mortar		8.18	3.26	0.084	0.042	31
	Print	Mortar	V.U	8.46	3.06	0.112	0.065	32
	Print	Mortar	W.U	8.29	3.39	0.104	0.057	31
	Print	Mortar	U.W	6.50	2.86	0.111	0.060	30
	Cast	Concrete		6.52	2.79	0.090	0.035	5
	Print	Concrete	V.U	8.48	1.13	0.117	0.055	4
	Print	Concrete	W.U	8.03	1.63	0.095	0.052	4
	Print	Concrete	U.W	5.37	2.25	0.104	0.048	4
4-Point bending test	Cast	Mortar		6.61	1.82	0.098	0.040	18
	Print	Mortar	W.U	6.91	0.00	0.073	0.000	1
	Print	Mortar	U.W	4.94	2.22	0.133	0.072	21
	Cast	Concrete		7.56	2.69	0.120	0.051	5
	Print	Concrete	V.U	9.20	0.00	0.058	0.000	1
	Print	Concrete	U.W	5.72	1.40	0.206	0.137	3
Splitting tensile test	Cast	Mortar		4.00	1.36	0.101	0.054	16
	Print	Mortar	V/W & V.U/W	3.55	1.39	0.167	0.106	19
	Print	Mortar	U/V & U.W/V	3.72	1.50	0.162	0.102	19
	Print	Mortar	W/U & W.U/V	3.29	1.26	0.157	0.073	17
	Cast	Concrete		3.49	0.75	0.064	0.027	4
	Print	Concrete	V/W & V.U/W	3.09	0.75	0.111	0.047	4
	Print	Concrete	U/V & U.W/V	3.62	0.24	0.042	0.021	3
	Print	Concrete	W/U & W.U/V	2.69	0.39	0.081	0.045	4
Uniaxial tensile test	Cast	Mortar		1.87	0.41	0.278	0.234	3
	Print	Mortar	W	2.40	0.92	0.142	0.077	3
	Print	Mortar	U	1.21	0.46	0.171	0.077	3
	Cast	Concrete		2.19	1.07	0.080	0.040	2
	Print	Concrete	W	3.35	0.00	0.196	0.000	1
	Print	Concrete	U	1.03	0.00	0.300	0.000	1

are averaged across all flexural and tensile test types as covered in this contribution, since the specimens are taken from the same printed or cast elements.

3.1 First observations

Across all test results, the various printing strategies are quite well represented, considering both continuous and batch printing processes. In terms of material strategies, both commercial and self-prepared mixtures have been used frequently, whereas the labs adopting a '2 K' mixture are underrepresented (only 3 unique lab-material combinations in this contribution). This should be kept in mind when considering the analyses of results.

In terms of labs per test, however, not all test types are well represented. The majority of available data concerns 3-Point bending, 4-Point bending, and splitting tests performed on mortar scale specimens. These tests have been performed on concrete scale as well, but to a significantly lesser extent. For uniaxial tensile testing, data is limited for both specimen scales. The analyses in the subsequent sections will therefore focus mainly on topics where sufficient data is available, to provide generalizable conclusions or recommendations.

Table 3 Results for the Dev1 (increased time interval) tests. The ratio between the average strength for printed specimens prepared with 'Dev1' settings to the Default cast specimens, both obtained by 3-point bending tests, is reported

Test type	Preparation	Scale	Orientation	Lab ID	Dev1 – Interval time [min]	Dev1 / Cast strength [–]	*n* Data
3-Point bending test	Print	Mortar	V.U	Lab12	0.5	1.17	5
	Print	Mortar	V.U	Lab15	20	0.82	5
	Print	Mortar	V.U	Lab20	20	1.16	6
	Print	Mortar	V.U	Lab30	30	1.00	3
	Print	Mortar	V.U	Lab13	60	0.91	5
	Print	Mortar	V.U	Lab01	95	0.71	7
	Print	Mortar	W.U	Lab12	0.5	1.17	5
	Print	Mortar	W.U	Lab15	20	0.96	5
	Print	Mortar	W.U	Lab20	20	1.13	6
	Print	Mortar	W.U	Lab30	30	1.29	3
	Print	Mortar	W.U	Lab13	60	0.88	5
	Print	Mortar	W.U	Lab01	95	0.83	7
	Print	Mortar	U.W	Lab12	0.5	0.99	5
	Print	Mortar	U.W	Lab15	20	0.22	5
	Print	Mortar	U.W	Lab30	30	0.61	3
	Print	Mortar	U.W	Lab13	60	0.62	5
	Print	Mortar	U.W	Lab01	95	0.27	7
	Print	Concrete	U.W	Lab30	30	0.49	5

From this first compilation of results (Table 2), it can be observed that the average 'tensile' strength range of printable cementitious materials across all participants is typically in the order of magnitude of 3–9 MPa, based on cast samples of mortar scale loaded in bending or splitting tests. Compared to the average compressive strength obtained on cast samples (58 MPa), this implies a ratio of approximately 5 to 16%, which is line with ratios reported by various studies covering a wide range of mix designs [21, 22]. At first glance, however, there is a clear differentiation in average strength values between the different types of tensile tests, both for cast and printed specimens, where uniaxial tensile results < splitting test results < flexural results. In contrast, no major differences in the strength values obtained at different scales, i.e., mortar or concrete, can be directly noticed from the results. A detailed discussion on the influence of and differences between test types and specimen scale will be provided in the analysis section.

For most test types performed on default process settings, the average number of valid specimens *n* per lab is at least equal to 5, which means that the exclusion of contributions based on too little data points ($n < 3$) is limited. Excluded outliers (individual specimens), are present infrequently in both printed and cast series—no clear differentiation is present, nor is there any apparent link between outliers and adopted material or printing parameters (see also Table 7 in the appendix). Similarly, the average CV across all labs (as reported in Table 2) varies considerably and does not show a clear dependency on preparation (print or cast), test type, or even number of participating labs for a particular test at first glance. This will be subjected to a more detailed analysis in the next section.

While the effect of deviations in printing process (Dev1, time interval) or curing conditions (Dev2) on strength appears to be considerable, as observed by strength ratios << 1.0 or >> 1.0 in Tables 3 and 4, no clear trend can be determined from the compiled results, since the applied deviations vary considerably between labs. These results will be studied in detail in the analysis section.

Finally, as seen from Table 4, the average density values of the tested printable material compositions

Table 4 Results for the Dev2 (variation in curing condition) tests. The ratio between the average strength for printed specimens prepared with 'Dev2' settings to the Default printed specimens, both obtained by 3-point bending tests, is reported

Test type	Preparation	Scale	Orientation	Lab ID	Dev2 / Default strength [-]	*n* Data
3-Point bending test	Cast	Mortar		7	1.16	5
	Cast	Mortar		22	0.53	5
	Cast	Mortar		23	1.10	4
	Cast	Mortar		27	0.99	5
	Print	Mortar	V.U	5	0.99	5
	Print	Mortar	V.U	6	0.84	6
	Print	Mortar	V.U	7	0.93	5
	Print	Mortar	V.U	9	0.76	5
	Print	Mortar	V.U	13	0.92	5
	Print	Mortar	V.U	19	1.19	6
	Print	Mortar	V.U	20	0.95	6
	Print	Mortar	V.U	22	0.76	5
	Print	Mortar	V.U	23	1.04	6
	Print	Mortar	V.U	24	1.25	4
	Print	Mortar	V.U	25	0.78	5
	Print	Mortar	V.U	27	1.71	5
	Print	Mortar	W.U	5	1.02	5
	Print	Mortar	W.U	6	0.84	5
	Print	Mortar	W.U	7	0.77	5
	Print	Mortar	W.U	9	0.77	5
	Print	Mortar	W.U	13	0.86	5
	Print	Mortar	W.U	19	1.08	6
	Print	Mortar	W.U	20	0.93	6
	Print	Mortar	W.U	22	0.56	5
	Print	Mortar	W.U	23	1.21	6
	Print	Mortar	W.U	24	1.00	5
	Print	Mortar	W.U	25	0.93	5
	Print	Mortar	W.U	27	2.39	5
	Print	Mortar	U.W	5	0.85	5
	Print	Mortar	U.W	7	0.93	5
	Print	Mortar	U.W	9	0.53	4
	Print	Mortar	U.W	13	0.81	5
	Print	Mortar	U.W	19	0.60	5
	Print	Mortar	U.W	22	0.48	5
	Print	Mortar	U.W	23	1.17	7
	Print	Mortar	U.W	24	1.34	5
	Print	Mortar	U.W	25	0.82	5
	Print	Mortar	U.W	27	1.82	5

centre around 2100 kg/m^3, and do not appear to vary much between scale (mortar or concrete) or the way the samples have been produced (casting or printing).

4 Analysis of results

This section provides an analysis of the experimental results. Firstly, the procedures to derive correlations between data points and exclude potential outliers is presented. These procedures have been applied

Table 5 Description of curing conditions for Dev2 tests

Lab ID	Dev2 – Curing Condition
5	Stored in climatic room (20 ± 2 °C and 60 ± 10% RH)
6	Unprotected after first day (21 ± 2 °C and 40 ± 10% RH)
7	Unprotected after first day (17–19 °C and 30–60% RH)
9	Unprotected after first day (21 ± 2 °C and 40 ± 10% RH)
13	Unprotected during the first day of curing only (20 ± 1 °C and 60 ± 5% RH)
19	Sprayed with water on the 1st day and then stored unprotected in climatic room (28 ± 2 °C and 60 ± 10% RH)
20	70 °C water bath for first 3 days; then water bath at 20 °C
22	Stored in climatic room (20 ± 0.5 °C and 50 ± 5% RH)
23	Stored in climatic room (20 °C and 65% RH)
24	Water bath curing up to 91 days under default conditions
25	Unprotected (23 ± 1 °C and 40 ± 10% RH)
27	Unprotected (21–24 °C and 40–50% RH)

throughout all of the following analyses and discussions. The corresponding visualization in graphical format is also explained, which is uniform throughout this section. Subsequently, the flexural and tensile strength properties of printed concrete are discussed, by considering the various tests types, cast or printed samples, the tested orientations, specimen size, effects of process deviations, and level of variability.

4.1 Procedure and visualization

The relationship between two sets of data points (e.g., cast samples versus printed samples) is analysed in the following subsections and visualised in the corresponding graphs. Here, it should be noted that these correlations are derived based on the assumption of linearity. For conventional concrete, this assumption is not necessarily applicable and non-linear relations have been accepted (e.g., in Eurocode, *fib* Model code). However, in the absence of such established relations for 3D printing, this provides a first, straightforward means to systematically evaluate the mechanical properties of printable concrete.

Table 6 Density results for the specimens across all labs

Preparation	Scale	μ Density [kg/m3]	σ Density [kg/m3]	n Labs
Cast	Mortar	2132	204	29
Print	Mortar	2108	189	30
Cast	Concrete	2155	127	7
Print	Concrete	2176	85	7

The respective average values of each lab are used to perform the analyses, which are indicated by the blue dots in the subsequent graphs. Firstly, linear regression is applied to these values using the least squares method. It can be expected that the resulting best fit line crosses the origin of the ordinate and abscissa (for instance, when the compressive strength reaches 0 MPa, the tensile strength will also be 0 MPa). However, these simple regression models often yield notable intercept values, in particular when data is scarce. To address this, proportionality is enforced for the remainder of the analyses.

The proportional best fit line is obtained by computing a linear regression line without an intercept value. Then, Cook's distance D is computed for each data point (i.e., lab), and the particular point is excluded from further analysis when $D > 1.0$, which indicates that this point excessively influences the slope of the regression line. These excluded points will be highlighted by a red diamond shape. For the remaining data points, this proportional line is recomputed, and any data point which exceeds two times the standard deviation of the residuals is also excluded from further analysis. These points will be highlighted by a red square shape. For the remaining data points, a new best fit is computed for a final time, still assuming proportionality between the two sets, which is represented by the continuous black line. The goodness of fit is evaluated through the R_0^2 value, and the slope k and standard deviation σ are reported. The slope value k may be considered as

the 'ratio' between the two data sets. Grey dots indicate data points (i.e., labs) that have been excluded a-priori, because the number of individual samples to compute (one of) the average value(s) was lower than 3, or because the age difference between the two strength values considered was larger than 11% (cf. Section 2). These points have not been included in the analyses. As a reference, the best fit line of the final data points, without the enforced proportionality, is plotted as well (dashed blue line), along with the corresponding goodness of fit (R_i^2 value) and level of statistical significance, where one, two, or three stars (*, **, ***) indicate <0.05, <0.01, and <0.001, respectively.

To express the goodness of fit, the R^2 values will be frequently referred to in the following sections. It can be debated which level these values should reach, for a relation to be considered meaningful. In this study, where the data points represent unique labs with unique material compositions, printer systems, and testing equipment, the following ranges are defined. $R^2<0.25$ are considered as low correlations, whereas $0.25<R^2<0.5$ are considered as moderate correlations. $0.5<R^2<0.75$ are high correlations, and $R^2>0.75$ are deemed as very high.

4.2 Influence of test type

Firstly, the ratio between compression tests and the four types of flexural and tensile tests is considered, based on cast specimens of 'mortar' scale, illustrated in Fig. 5. The results of F3P and STT show a moderate to high significant correlation between their respective flexural or tensile strength values and the compressive strength. In both cases, the best fit is almost identical to the line of proportionality. While it is generally seen in most engineering standards that the tensile strength variation is presented in terms of the square root of the compressive strength, in the current case, a linear relationship is considered in the absence of any prior evidence to the contrary. For the case of F4P, the correlation and significance is low, whereas for the UTT, the number of data points (i.e., labs which have performed this test) is simply too small to perform any meaningful statistical analysis.

The slope k of these proportional lines, i.e., the ratio between the two strength values, clearly varies between the test types. The highest ratio is obtained in the 3-point bending tests, where the average flexural strength is equal to approximately 15% of the compressive strength. This reduces to approximately 11% in 4-point bending, and finally to 7% for the splitting tests.

While the ratio obtained in F4P tests should be considered carefully, given the low R^2 values and significance, the observed trend between the tests, i.e., F3P > F4P > STT, is as expected and may be attributed to the different configurations. In a 3-Point bending test, the highest bending stresses occur (locally) directly underneath the loading introduction, whereas in the case of a 4-Point bending or splitting test, a larger region with (almost) constant maximal state of stress is present. For a heterogeneous material like

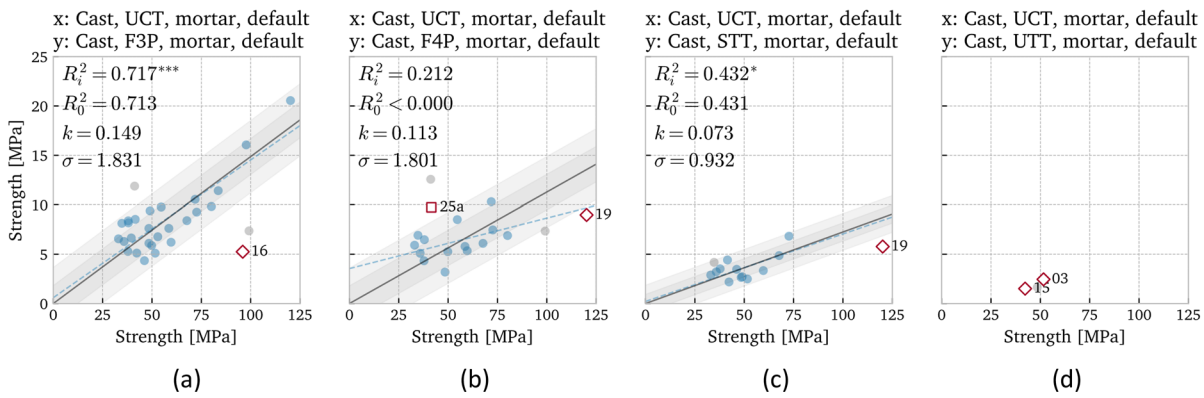

Fig. 5 Correlation between compression strength and flexural or tensile strength obtained by 3-Point bending (**a**), 4-Point bending (**b**), splitting tensile (**c**), and uniaxial tensile tests (**d**), performed on cast specimens of 'mortar' scale. The strength values plotted on x and y axes are declared at the top of each graph

concrete, this means that the probability to find the weakest material point (and thus the strength) is higher in F4P and STT compared to F3P. It should also be noted that the state of stress in each test setup is different, for instance, the span to depth ratio of F3P and F4P specimens represents a (mildly) deep beam, and the strength obtained is thus expected to deviate from what is measured in a uniaxial tensile test.

Next, the correlation between the various tests will be considered, for both cast and printed samples. Note that uniaxial tensile tests will be excluded from further analysis, from here onwards. For the printed samples, the loading orientations have been matched such that the layers are loaded in a similar manner (e.g., U.W in F3P is matched with W/U in STT), as illustrated in Fig. 6.

In most cases, a high to very high significant correlation between the two strength values considered is found, where the best fit line is very close to proportionality. Only for the case of cast F3P-STT and printed F3P V.U-STT V/W, considerable scatter results in a lower correlation. In other words, as long as the loading conditions with respect to the layers are matched, one type of tensile test can be used to compute the strength as obtained in another. The conversion between the two strengths, i.e., the ratio k, varies however significantly between printed and cast samples, as well as between the printed specimens loaded in various orientations. This will be analysed in the next section.

4.3 Influence of loading and specimen orientation

Figures 7 and 8 show the correlation between cast samples and printed samples obtained in F3P tests, for the various loading and specimen orientations. In all cases, a high to very high significant correlation

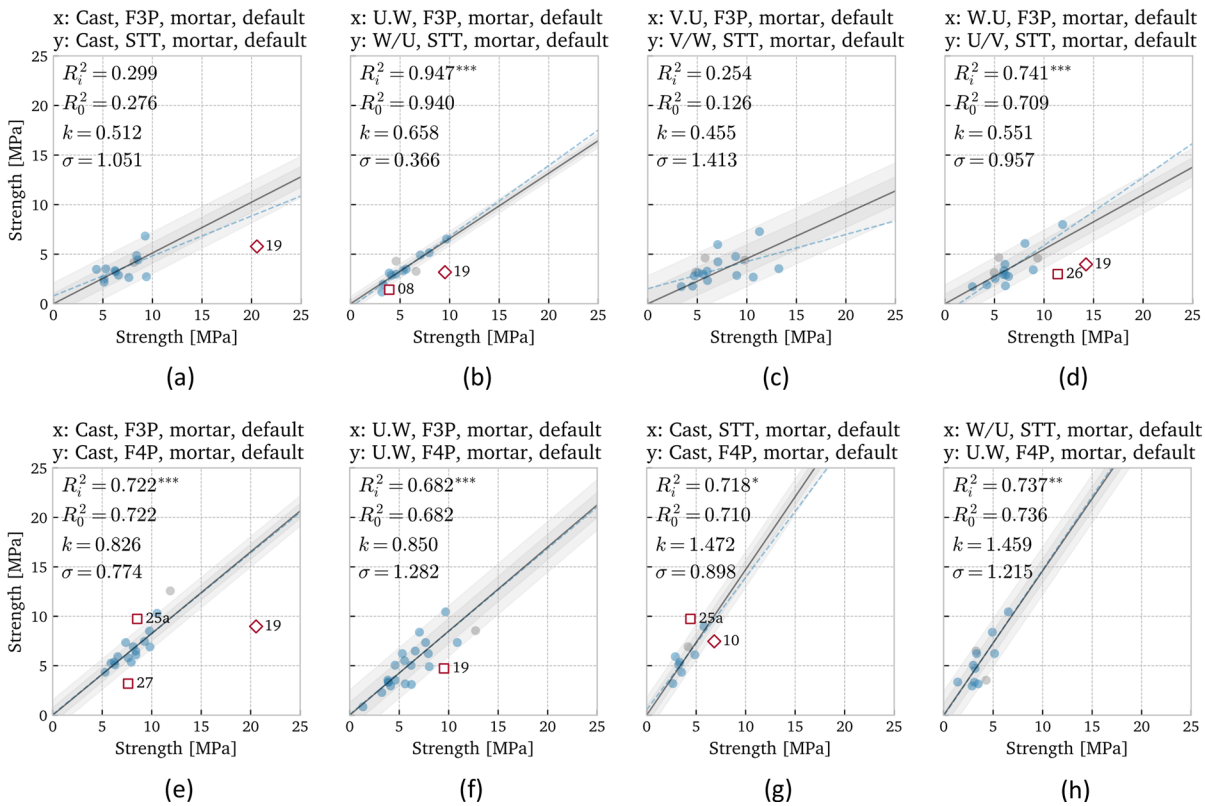

Fig. 6 Correlation between strength values obtained on printed and cast specimens of 'mortar' scale: 3-point bending results and splitting tensile results **a** to **d**, 3-point bending to 4-point bending results (**e**, **f**) and splitting tensile results to 4-point bending results (**g**, **h**). The strength values plotted on x and y axes are declared at the top of each graph

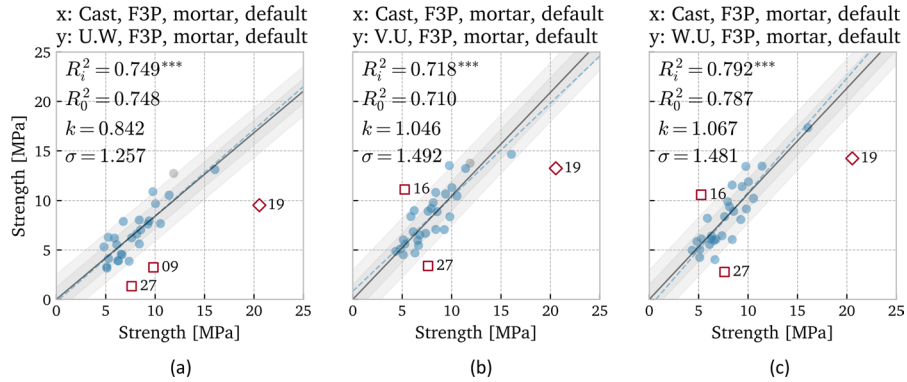

Fig. 7 Correlation between 3-point bending test results for cast specimens and printed specimens loaded in U.W (**a**), V.U (**b**), and W.U (**c**) orientation, 'mortar' scale. The strength values plotted on x and y axes are declared at the top of each graph

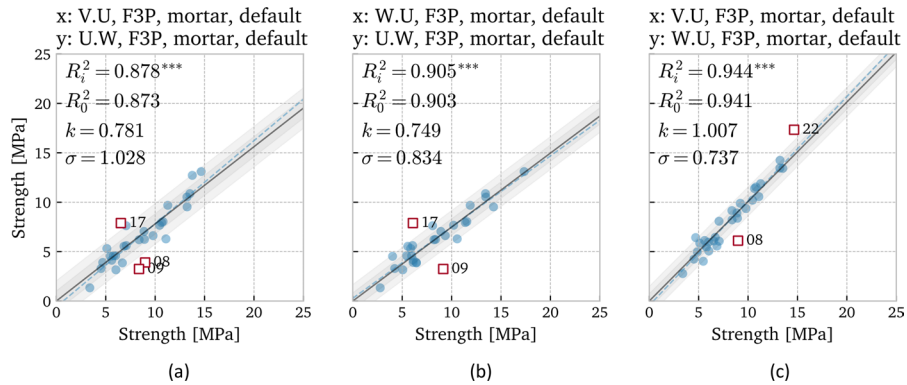

Fig. 8 Correlation between 3-point bending test results for printed specimens loaded in V.U and U.W (**a**), W.U and U.W (**b**), and V.U and W.U (**c**) orientation, 'mortar' scale. The strength values plotted on x and y axes are declared at the top of each graph

is found, where the best fit line is almost identical to the line of proportionality. Moreover, in the cases where the main tensile stresses are not acting perpendicular, but parallel to the layers (i.e., V.U and W.U), the strength values of the printed samples are almost identical and moreover also identical to those obtained in 'cast' specimens. This is indicated by the k values of approximately 1.0.

As the strength values of the cast specimens and printed specimens loaded in V.U. and W.U are (almost) identical for the case of F3P, these can be merged into one larger dataset, designated as 'Bulk' hereafter, which will enable a more sound statistical analysis on the correlation with the remaining, critical loading orientation U.W, perpendicular to the printed layers.

A similar approach is applied to the results of the STT performed on cast and printed samples, loaded in various orientations (Fig. 28 in the appendix). Here, the correlations found are similarly high to very high, and, although the k values deviate slightly more from 1.0 when including the cast specimens, the cast samples and the printed samples where the layers are loaded in parallel (V/W & V.U/W, and U/V & U.W/V) can be considered as approximately identical. These values are therefore also merged into one 'Bulk' dataset. For the case of F4P, insufficient datapoints have been collected to perform a similar procedure.

Now that two larger, new datasets have been created, individual outliers can be better detected and excluded following the procedure discussed in Sect. 3 (illustrated in Figs. 26 and 27 in the appendix). The remaining datapoints can be used to define the influence of the layer interface in 3D printed concrete, by comparing the 'bulk' strength to the U.W strength for F3P and to the W/U & W.U/V strength for STT, as illustrated in Fig. 9. Again, a very high significant correlation is found, which highly approximates proportionality. The obtained strength when the tensile stresses are acting perpendicular to the layers, is

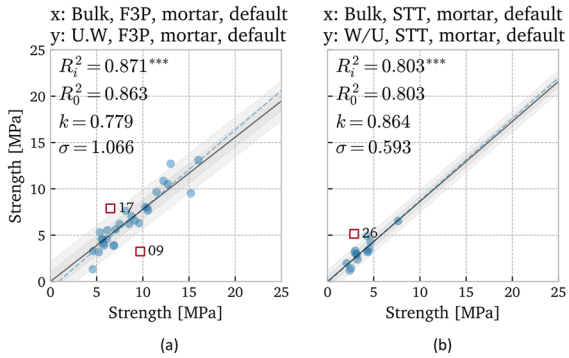

Fig. 9 Correlation between 'bulk' results and specimens loaded in U.W (F3P) (**a**) or W/U & W.U/V (STT) orientation (**b**). The strength values plotted on x and y axes are declared at the top of each graph

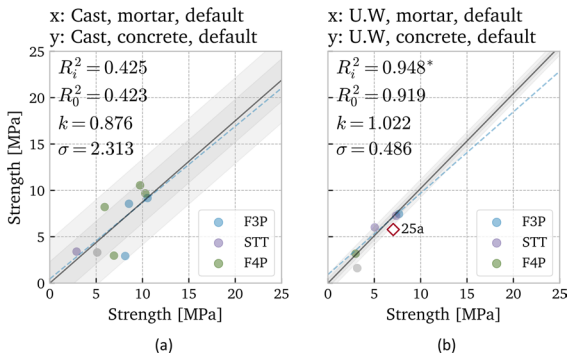

Fig. 10 Correlation between 'mortar' and 'concrete' scale strength values on cast samples (**a**) and printed samples loaded in U.W orientation (**b**). The three different colour dots indicate three different test types (F3P, STT, and F4P). The strength values plotted on x and y axes are declared at the top of each graph

approximately 78% of the bulk strength in the case of 3-point bending, and 86% for splitting tests.

4.4 Influence of specimen size

To analyse the influence of specimen size, the strengths obtained on 'mortar' scale will be compared to those obtained on 'concrete' scale specimens (cf. dimensions in Table 1). The number of laboratories who have performed two identical tests on both scale is, however, limited. To provide a first insight nevertheless, the different test types (F3P, F4P, and STT) will be merged into one correlation plot. The procedure and visualization as elaborated in Sect. 4.1 is adopted, with the addition of different colours for each test type: blue dots for F3P, purple dots for STT, and green dots for F4P, see Fig. 10.

For cast specimens, a moderate correlation is observed, although care should be taken given the significance of this correlation. The ratio k equal to approximately 0.9, implies a 10% strength reduction of 'concrete' scale specimens, compared to 'mortar' size. This decrease in strength as the specimen size increases is in line with observations obtained by both direct and indirect tensile testing [21, 23, 24].

This reduction is however not apparent for printed specimens, where a very high significant correlation is observed for the specimens loaded in U.W orientation (the other orientations do not have sufficient data points), with k approximately equal to 1.0. This might be attributed to the presence of layer interfaces loaded perpendicular in this orientation. Independent of the size of the specimen, this interface is the 'weakest' link and will fail before the 'bulk' strength is exceeded (cf. the previous section). It should be noted that the number of data points for this analysis is limited, and a much larger dataset is required to reinforce this observation, and moreover, provide similar analyses for the other loading orientations.

4.5 Influence of source location

To define the influence of source location of specimen extraction, the specimens tested in STT on mortar scale can be considered, as they have been extracted from thee different locations in a printed wall element (bottom, middle, top). This is illustrated in Fig. 11, where a very high significant correlation is found between all locations considered, approximating proportionality. As implied by k close to 1.0, the strength obtained by specimens taken from top and middle locations are almost identical. A minor reduction (roughly 5–10%) in strength is observed in specimens taken from the bottom location. No variation of density was observed between the three locations (k equal to 1.0 in Fig. 30 in the Appendix). A potential explanation for the strength reduction

could therefor reside in local disturbances caused by the printing process or specimen preparation (e.g., extraction or sawing) near the bottom surface. This requires, however, further study for confirmation.

4.6 Density

The density of cast and printed default specimens is compared, on both 'mortar' and 'concrete' specimen scale. As illustrated in Fig. 12, very high significant correlations are found for both individual scales, with a k value close to 1.0. This also applies to the comparison of printed mortar to printed concrete scale specimens, although here the best fit line deviates somewhat from proportionality. Simply put, on average the density does not change between printing or casting, independent of the specimen size, given default process settings.

4.7 Influence of an increased time interval (Dev1)

To determine the influence of an increased time interval between layers on the strength properties of 3D printed concrete, the results of the F3P performed on mortar scale specimens, as summarized in Table 3, will be analysed. This is the only loading configuration that has been tested by multiple participants. Even in this configuration, the available data is limited, and it should moreover be noted that each laboratory has individually selected the time interval value corresponding to their particular material and 3D printing system, which thus varies across the results (from 0.5 min. up to 90 min.). For the subsequent analysis, the Dev1 results of Lab12 will not be included, since the adopted increased time interval (0.5 min.) is approximately identical to the default process settings.

Across all Dev1 results of F3P mortar scale specimens, a clear reduction in flexural strength is apparent

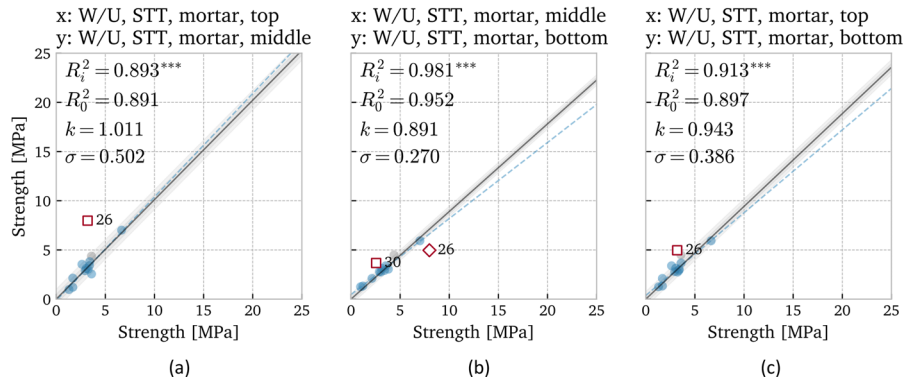

Fig. 11 Correlation between splitting tensile test results for printed specimens loaded in W/U & W.U/V orientation, 'mortar' scale, subtracted from top and middle (**a**), middle and bottom (**b**), and top and bottom (**c**) locations. The strength values plotted on x and y axes are declared at the top of each graph

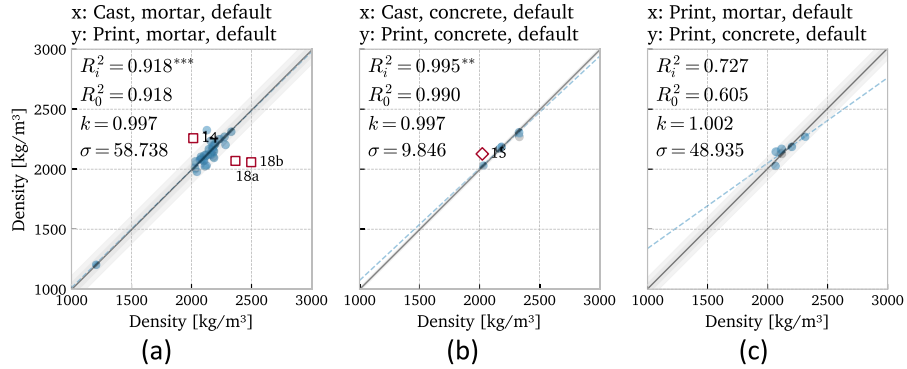

Fig. 12 Correlation between 'density' values of cast and printed specimens, on mortar (**a**), concrete (**b**) and both (**c**) scales. The values are computed based on all included specimens subjected to a flexural or tensile test. The density values plotted on x and y axes are declared at the top of each graph

in the 'weakest' loading orientation U.W, i.e., where the main (flexural) tensile stresses are acting perpendicular to interfaces between layers, compared to the strength obtained on default, cast specimens. This reduction ranges from −78% (lab15, 20 min.) to −38% (lab13, 60 min.) Lab15 makes use of a 2 K printing material, which results in a significant reduction of strength, even with a moderately increased time interval. In comparison, Lab01, with a 1 K printing material, obtained a similar strength reduction (−73%), after 95 min of increased time interval.

For the majority of Dev1 results, no flexural strength reduction is observed for the other two loading orientations V.U and W.U. In fact, for some participants a minor to moderate increase was reported. Only for Lab01 (95 min.), a strength reduction of -29% and -17% was found for F3P specimens loaded in V.U and W.U orientation, respectively. This reduction is moderate compared to the -73% strength in W.U orientation, but nevertheless significant.

The effect of an increased time interval depends on the material composition, printing strategy, and environmental conditions during printing. It is therefore not possible to formulate a universal reduction factor to take this effect into account, based on the results of this ILS only. The strength reduction can however be considerable and is most apparent in U.W loading orientation. If an increased time interval is inevitable in a 3D printing project, it can be recommended to assess at least the strength properties in this loading orientation under representable printing conditions.

4.8 Influence of a variation in curing condition (Dev2)

To determine the influence of different curing conditions on the flexural and tensile properties of 3D printed concrete, the F3P results and conditions as summarized in Tables 4 and 5 are analysed. The number of participating labs with similar conditions is, however, very limited. Participants have generally opted to deviate from default curing (storing in a water tank), by storing their samples in a climate controlled room instead, or to leave their samples unprotected until testing. The exact conditions (i.e., temperature and relative humidity), moreover varied between labs. Hence, the following observations cannot be seen as an exact trend, but provide a starting point for further studies on the effect of curing conditions.

For the climate controlled specimens, two out of four participants (ID5 and ID23) found limited influence of the variation in curing condition compared to curing in a water tank (default curing), as observed by the strength ratios close to 1.0. One participant (ID22), however, obtained significant reduction in F3P strength for all orientations, up to -52% in the U.W loading orientation, while for another (ID19) this reduction was only present (-40%) in the U.W orientation. For the unprotected specimens (ID6, ID7, ID9, ID13, ID25 and ID27), this type of less-controlled curing generally leads to a modest reduction of strength compared to default curing, as observed by the ratios in the range of approximately 0.70 to 0.90 across all loading orientations considered. Surprisingly, one participant of unprotected specimens (ID27) found significant strength increases (up to +140% in W.U orientation), compared to curing in a water tank, whereas this increase was not present at all in the case of cast specimens (ratio almost equal to 1.0).

Given this strongly diverging effect of varying curing conditions on the strength values, no definite conclusions can be drawn based on the results of this ILS, although the majority of data indicates that uncontrolled curing reduces the strength in all loading orientations. In anticipation of further studies on this topic, for 3DCP projects in practice, it can be recommended that test specimens are cured in representative conditions, to avoid over- or underestimation of strength properties.

4.9 Discussion of variability

The variability of the printed and cast specimens is analysed based on the data obtained from default mortar scale specimens only, due to limited availability of data points on concrete scale. The procedure and visualization are identical to the previous sections, where now the average coefficient of variation (CV) will be discussed and visualized, rather than the average strength values. The correlation plots for specimens subjected to different test procedures, loading orientations, and preparation (cast or print), are shown in Appendix Fig. 31, 32, 33 and 34.

At first, the variability of flexural, splitting and compression tests are compared based on cast samples. In all cases the tests considered (F3P, F4P, and STT) show a higher CV than compression test ($k > 1$), but the significance and correlation is low – with the exception of STT. This may be attributed to the presence of voids in the cast specimen, which is a primary attribute for failure in tensile tests. This characteristic has, however, not been recorded in this ILS-mech and cannot be analysed in detail.

When comparing the variability between tests, on both cast and printed (matching orientations) samples, F3P shows consistently considerable higher CV than STT. Although, again, it should be noted that the significance and correlation are low due to considerable scatter. In contrast, the variability in F3P and F4P results are much more similar (k close to 1.0), while comparison between F4P and STT leads to no meaningful results (considerable scatter and much less datapoints). This difference in variability could be explained by the extraction procedure and state of stress during testing, which is much more similar for F3P and F4P (e.g., maximal stress at the bottom edges of the specimens), but differs from STT specimens (e.g., maximal stress in the mid-region), and requires further investigation regarding the effect of local defects, void distribution and layer orientation.

No significant correlations can be observed when comparing the coefficient of variation of the various 'printed' orientations with 'cast' samples for the case of F3P (high scatter) and STT (data scarcity). When comparing 'print' to 'print' orientations, for F3P, these correlations are moderate: it appears that the variability is consistently lower when specimens are loaded in the 'critical' U.W orientation. Since failure typically occurs in the interface between layers, the variability can be expected to be lower than the cases where either the interface or the bulk can fail.

From this section, it is inferred that the variability in flexural or tensile strength is dependent on the interface properties and on the test type. The variation observed for one specific orientation for one specific test may not correlate at all with the other specific orientation or other specific test. The sampling size also needs to be increased to reduce the variability in results, especially for the cases where the failure plane is not certain.

4.9.1 Analysis of outliers

Finally, the outliers which are present throughout the strength correlation plots discussed in Sects. 4.2 to 4.4 are analysed, to find potential reasons for frequent deviation from the generally observed trends. The number of times a laboratory is observed to be an 'outlier' is summarized in appendix Table 8, along with the relevant material and printing parameters of that lab.

In total 12 labs, out of 30 labs, are outlier in one case or another. Lab 19 is observed to be outlier in 10 cases, which is the most of all labs. The major reason appears to be the high compressive strength of the mix (120 MPa based on cast samples), which approximates 'ultra-high strength' concrete, resulting in a behaviour much different from the other labs which are in the normal to high strength range. However, it should be noted that lab 19 does not consistently outperform the other labs in terms of absolute strength values (as observed in the box plots in Sect. 3 and the appendix), while other labs reaching high strength values appear much less or not at all in the list of outliers. For the other labs, apart from lab 19, which appear multiple (3–4) times in the list of outliers, the adopted material and printing parameters vary over a wide range (e.g. aggregates sizes from 0.5 to 4 mm, and nozzle areas of 314 to 2100 sq. mm). It is therefore not possible to determine the critical parameters affecting their behaviour.

5 Conclusions

This contribution discusses the flexural and tensile strength properties of 3D printed concrete based on an extensive dataset collected during a RILEM 304-ADC Interlaboratory Study. The main findings of the analyses on the experimental results are summarized below. As a next step, the TC 304-ADC intends to develop RILEM Recommendations for testing of mechanical properties of 3D printed concrete based on the results of this study, and the evaluation of test methods, data sets and study plan [12–16].

- The ratio between the flexural or tensile strength and compressive strength varies between tests. Based on the simplest case considered, i.e.,

cast specimens of 'mortar' scale', the strength values followed the expected trend where F3P > F4P > STT. The exact ratios have to be further refined, as the soundness of the correlation in this study was limited, and have only been established based on cast samples, and may thus not be identical for printed samples.

- For printed samples, one type of flexural or tensile test can be used to compute the strength as obtained in another. This conversion varies between test types, specimen preparation, and loading to layer orientation. Thus, the orientation in which samples are printed and loaded should be carefully considered.
- For F3P and STT performed on mortar scale specimens, which concerns the majority of datapoints in this contribution, cast or printed samples show similar behaviour, as long as the main tensile stresses are acting parallel to the printed layers, i.e., V.U and V.W orientation (F3P) or V/W & V.U/W and U/V & U.W/V (STT). In these cases, on average, the tensile strength of printed concrete is approximately identical to cast material. A strength reduction occurs when the tensile stresses are acting perpendicular to the layers, and is found on average to be approximately 78% of the bulk strength in the case of 3-point bending, and 86% for splitting tests.
- No reduction is apparent between printed specimens of 'concrete' or 'mortar' scale, loaded in U.W orientation, although the number of data points for this analysis is very limited. The effect of specimen scale will require further consideration, especially also regarding the remaining loading to layer orientations, which was not possible based on the current dataset. On 'concrete' scale, this will introduce additional 'horizontal' interfaces in the specimens, as a result of which the equality found on 'mortar' scale between V.U and V.W orientations may no longer hold.
- The splitting strength obtained by specimens taken from top and middle locations are almost identical. A minor reduction (roughly 5–10%) in strength is observed in specimens taken from the bottom location.
- On average the density does not change between specimens obtained by printing or casting, and is found to be independent of the specimen size.
- The effect of an increased time interval between layers on the tensile strength can be considerable, and is most present in the 'critical' U.W loading orientation. Due to the dependency on material composition, printing strategy, and environmental conditions during printing, it is not possible to define a generic rule to take this effect into account, based on the result of this ILS only. In any case, if an increased time interval is inevitable in a 3D printing project, the strength properties should be characterized in (at least) this loading orientation under representable printing conditions.
- The effect of variation in curing condition (e.g., climate controlled storage or unprotected curing) can be pronounced, but the observed effects varied widely between participating laboratories, ranging from significant strength increase to large reduction. A general trend could not be derived and will require additional studies. It is therefore recommended to store test samples in representative curing conditions, compared to the 3D printing project of interest.
- From this study, it was found that the variability of strength values, expressed through a coefficient of variation, varies between test type, preparation, and loading orientation, but a straightforward correlation between the cases considered, could not be established.
- An effort was made to evaluate datasets which constituted outliers of the overall trend. With the exception of one case, it was not possible to define the critical parameters which causes deviations, due to the wide variety of mixtures and printing processes adopted. For the single case, the high compressive strength of the adopted mixture (> 120 MPa) was pinpointed as a potential reason. Verifying the analyses performed for this ILS, beyond the typical strength range of the affiliated dataset, is therefore strongly recommended before extrapolating these conclusions.

Finally, it should be emphasized here that all observations are based on the averages and trends across *all* participating laboratories. It is, however,

with the current knowledge not possible a-priori to define where a certain material composition or printing system is positioned. This means that the statistically significant quantitative correlations that have been observed over the entirety of participating laboratories, e.g., between cast and printed specimens, should not be used to determine engineering properties of materials from one specific laboratory without further consideration. Based on the current paper and [12–16], the development of recommendations regarding testing to obtain engineering properties will be part of the future work of RILEM TC 304-ADC.

Acknowledgements The authors express their sincere gratitude to all 30 laboratories that have contributed to this interlaboratory study and the associated persons, in particular: Carolina M. Rangel, Eric Wijen, Naomi van Hierden, Albanela Dulaj (Eindhoven University of Technology), Emre Ortemiz (ISTON), Zeynep Basaran Bundur (Ozyegin University), Jaime Mata-Falcón, Lukas Gebhard, Ana Anton, Che Wei Lin, Ming-Yang Wang (ETH Zurich), Rafael Pileggi (University of São Paulo), Amar Yahia, Masoud Hosseinpoor, Belkis Selma Aouichat, Yacine Hani Bouchilaoun, José Vidal Gonzalez Avina, Shahab Azizi (Université de Sherbrooke), Jiří Vambera (ICE Industrial Services), Tomaž Simon, Rafael Kajzer (Slovenian National Building and Civil Engineering Institute), Passarin Jongvisuttisun (SCG Thailand), Jay Sanjayan (Swinburne University of Technology), Dietmar Stephan (Technical University of Berlin), Steffen Müller (TUD Dresden University of Technology), Denisa Jancarikova (Research Institute for Building Materials, Czech Republic), James Dobrzanski, and Jie Xu (Loughborough University). Furthermore, the following research funding is gratefully acknowledged: National Key R&D Program of China (No. 2023YFC3806902) by author Zhao. Finally, the gracious supply of materials and/or use of facilities is appreciated of: Saint-Gobain Weber Beamix by authors Versteege and Wolfs, Istanbul Concrete Elements and Ready Mixed Concrete Factories (ISTON) by authors Ozturk and Ozyurt, PERI 3D Construction GmbH by authors Richter and Jungwirth, Heidelberg Materials by authors Bos, Auer, Hechtl and Dahlenburg.

Funding Open Access funding enabled and organized by Projekt DEAL.

Data availability The study plan for this interlaboratory study on mechanical properties of 3D printed concrete is publicly available as dataset [12] from mediaTUM at https://doi.org/https://doi.org/10.14459/2023mp1705940. The processed and selected results used for the analyses presented in this paper have been published as dataset on Zenodo [14] at https://doi.org/https://doi.org/10.5281/zenodo.12200570. This dataset is only available to participating laboratories until the embargo date 1.7.2025. After that, it will be publicly accessible.

Appendix

See Figs. 14, 13, 15, 16, 17, 18, 19, 20, 21, 22, 23, 24, 25, 26, 27, 28, 29, 30, 31, 32, 33, 34 and Tables 7, 8.

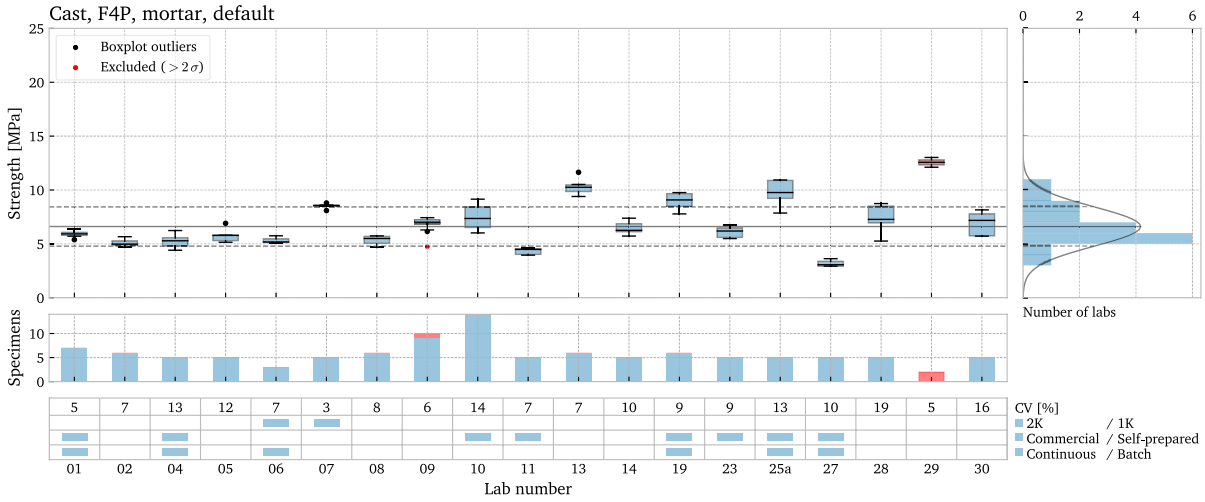

Fig. 13 Flexural strength values obtained by 4-Point bending tests performed on cast specimens of 'mortar' scale

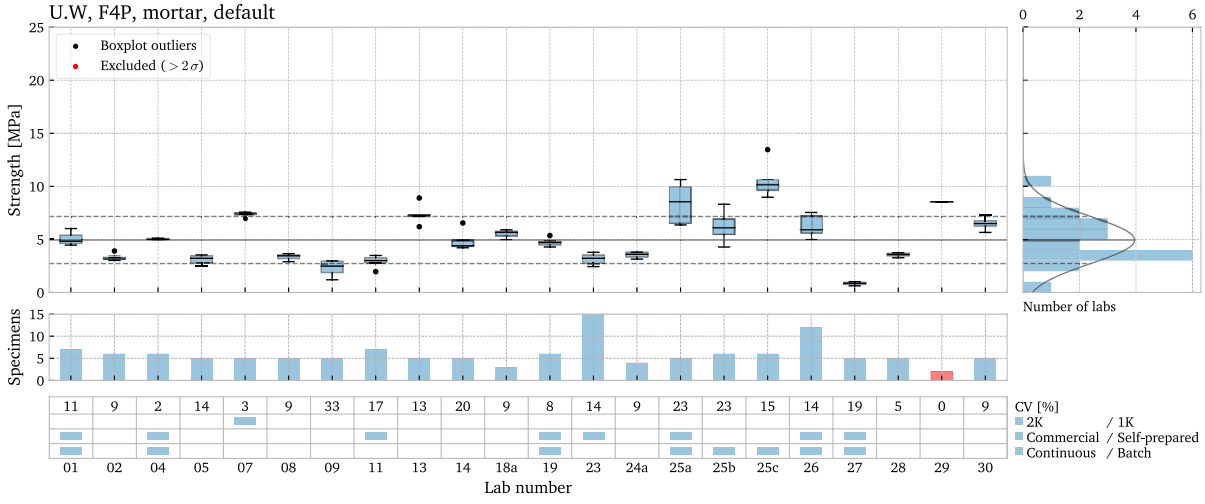

Fig. 14 Flexural strength values obtained by 4-Pont bending tests performed on printed specimens of 'mortar' scale, loaded in U.W orientation

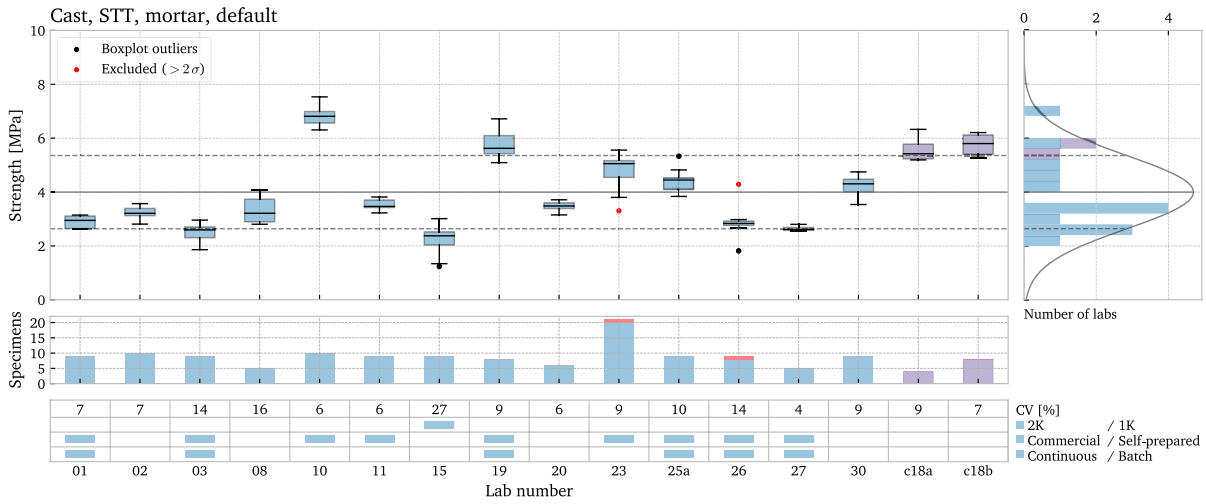

Fig. 15 Splitting tensile strength values obtained by splitting tests performed on cast specimens of 'mortar' scale

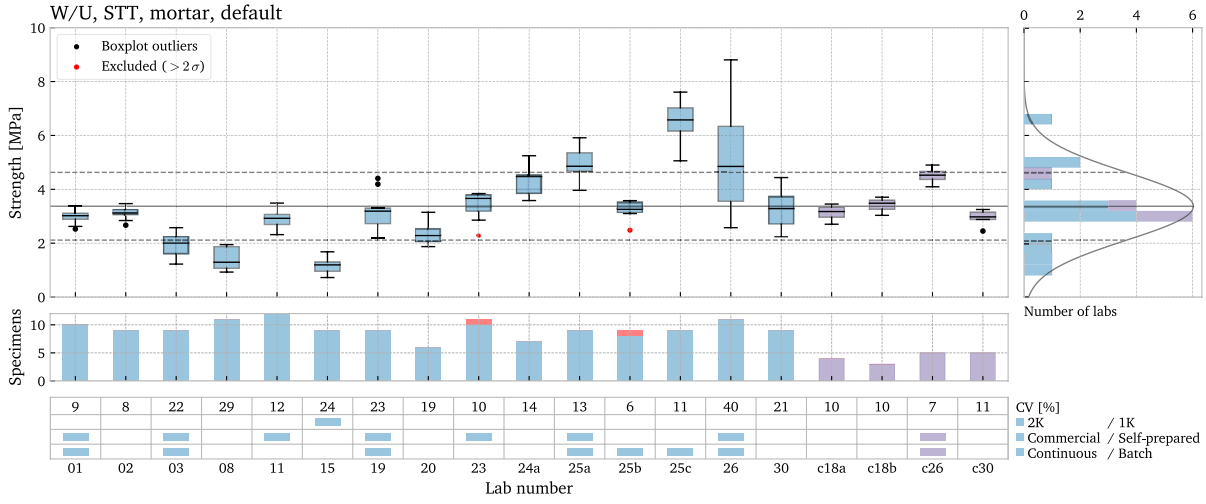

Fig. 16 Splitting tensile strength values obtained by splitting tests performed on printed specimens of 'mortar' scale, loaded in W/U (cubic, blue) or W.U/V (cylindrical, purple) orientation

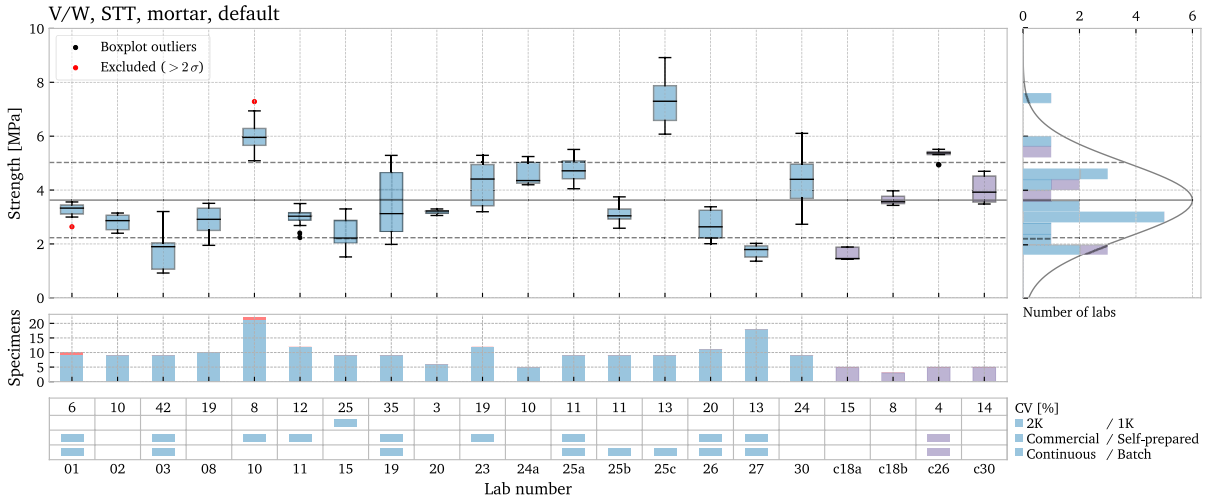

Fig. 17 Splitting tensile strength values obtained by splitting tests performed on printed specimens of 'mortar' scale, loaded in V/W (cubic, blue) or V.U/W (cylindrical, purple) orientation

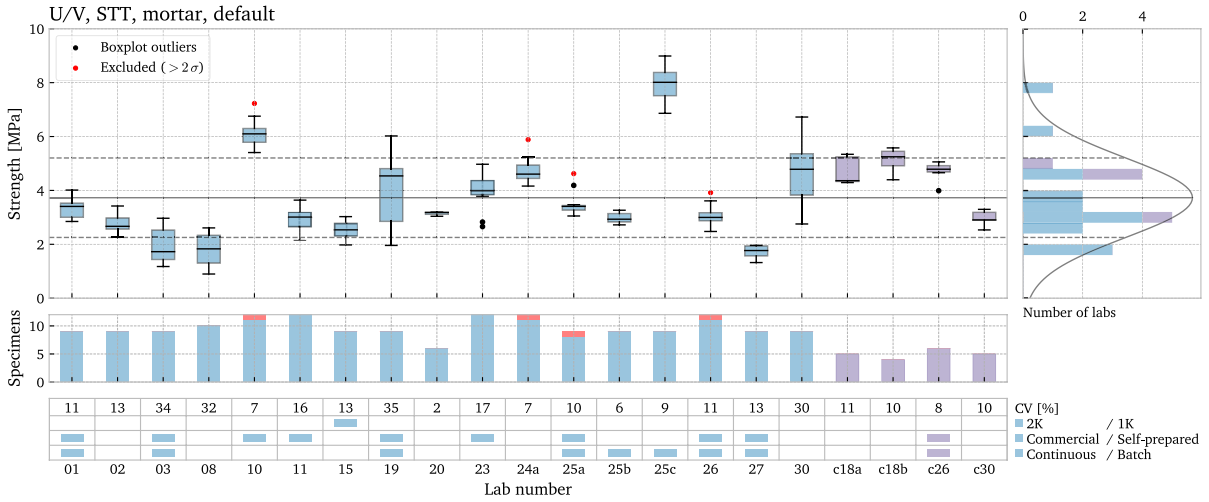

Fig. 18 Splitting tensile strength values obtained by splitting tests performed on printed specimens of 'mortar' scale, loaded in U/V (cubic, blue) or U.W/V (cylindrical, purple) orientation

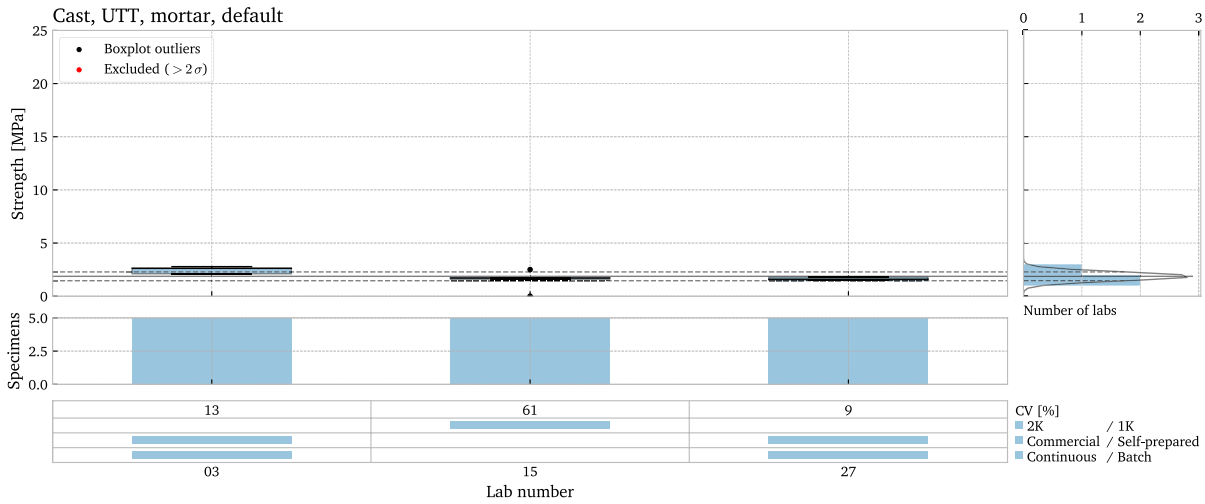

Fig. 19 Tensile strength values obtained by direct tensile tests performed on cast specimens of 'mortar' scale

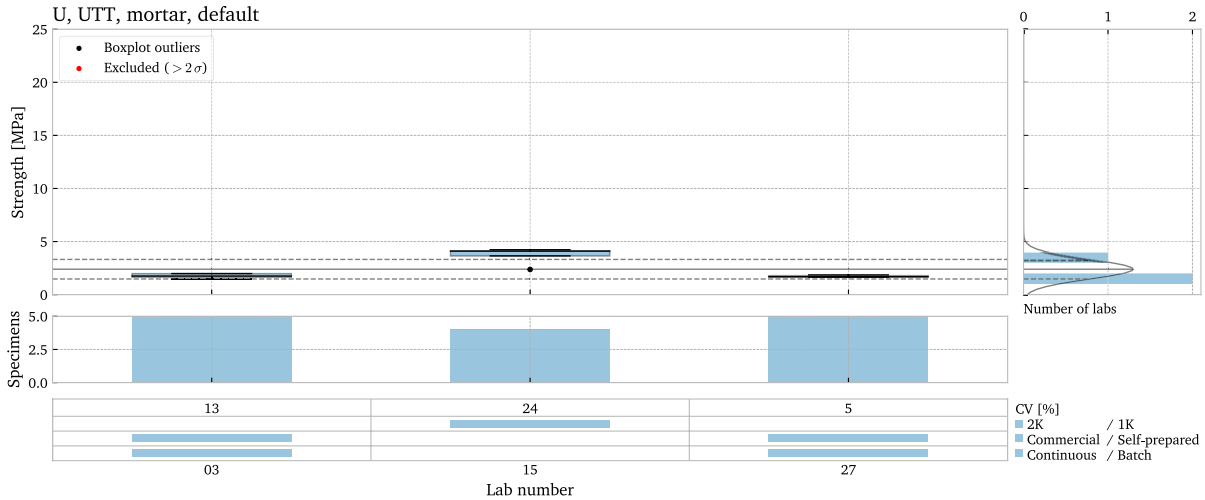

Fig. 20 Tensile strength values obtained by direct tensile tests performed on printed specimens of 'mortar' scale, loaded in U orientation

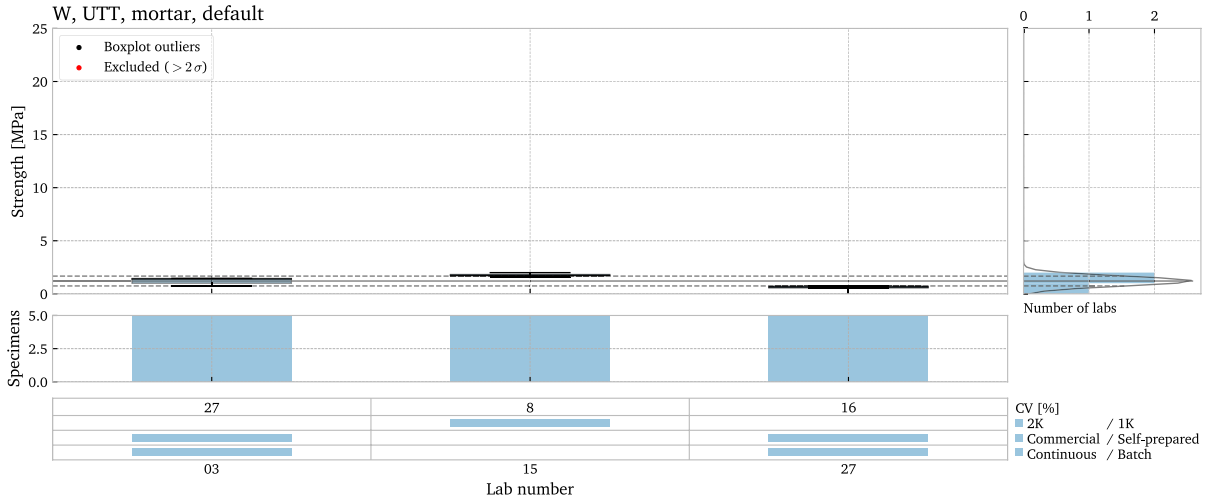

Fig. 21 Tensile strength values obtained by direct tensile tests performed on printed specimens of 'mortar' scale, loaded in W orientation

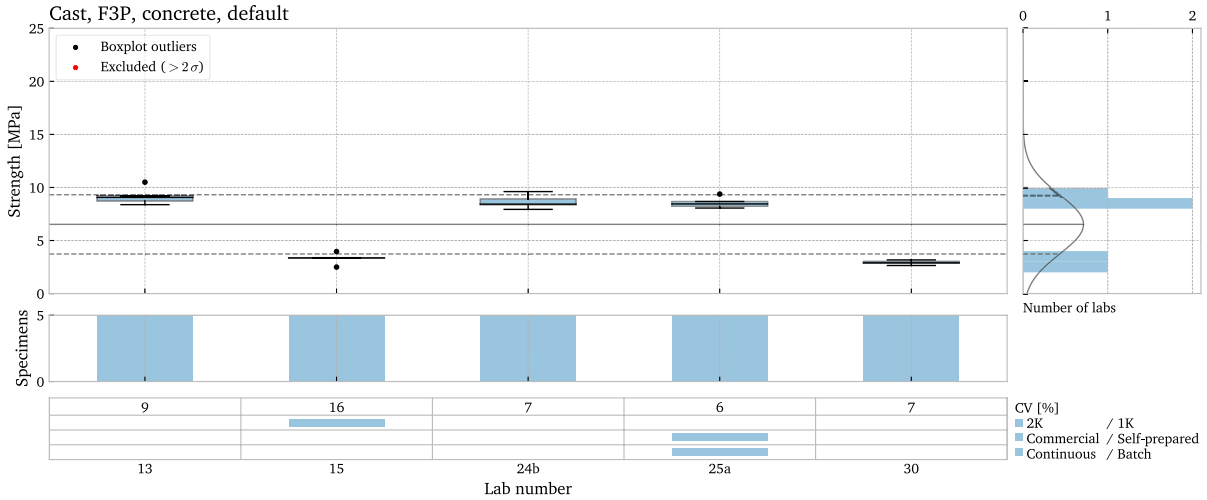

Fig. 22 Flexural strength values obtained by 3-Point bending tests performed on cast specimens of 'concrete' scale

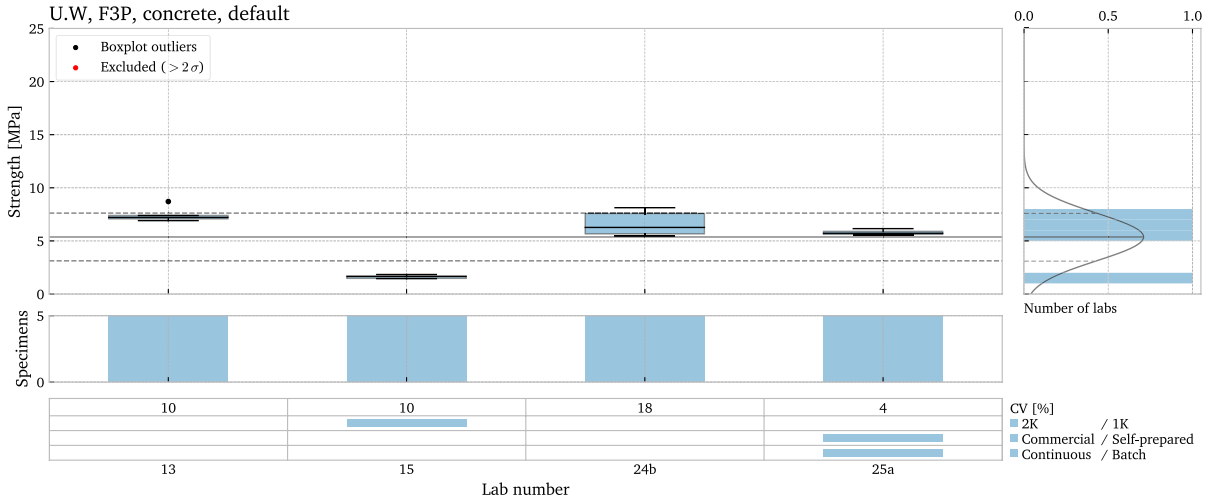

Fig. 23 Flexural strength values obtained by 3-Point bending tests performed on printed specimens of 'concrete' scale, loaded in U.W orientation

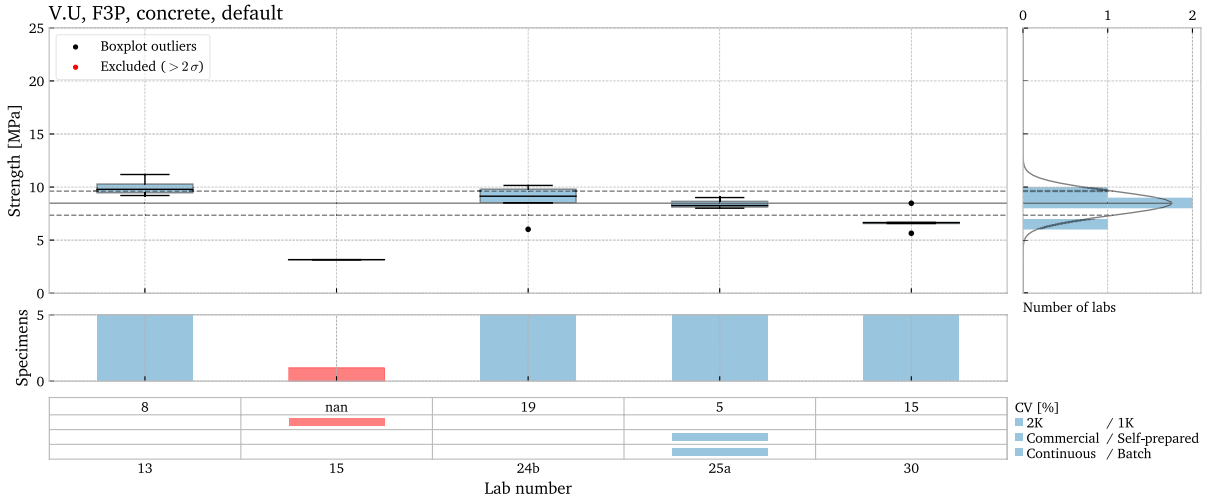

Fig. 24 Flexural strength values obtained by 3P bending tests performed on printed specimens of 'concrete' scale, loaded in V.U orientation

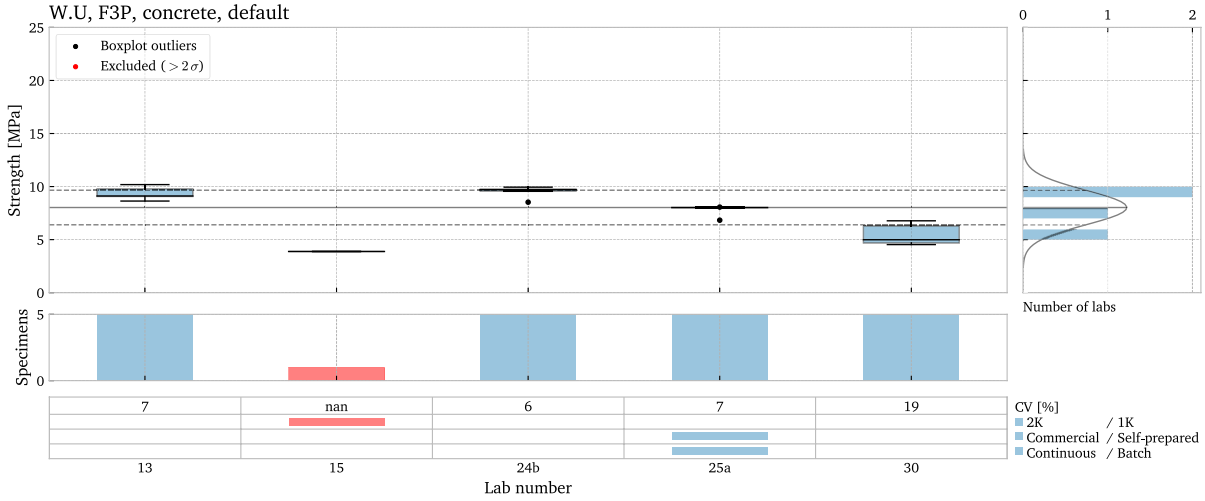

Fig. 25 Flexural strength values obtained by 3P bending tests performed on printed specimens of 'concrete' scale, loaded in W.U orientation

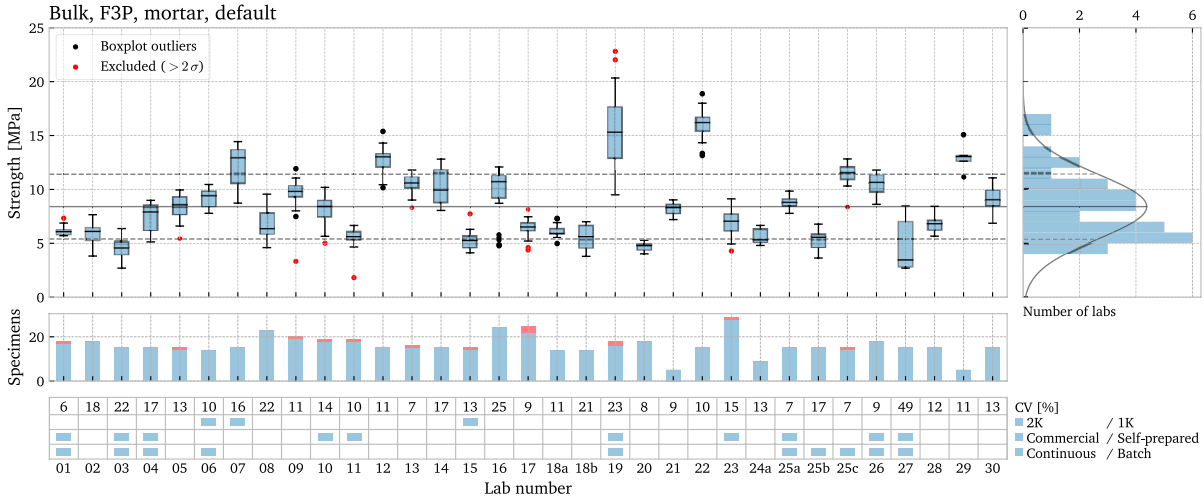

Fig. 26 Flexural strength values obtained by 3P bending tests performed on specimens of 'mortar' scale, for the 'bulk' orientation (combination of cast specimens and printed specimens loaded in V.U and W.U orientation)

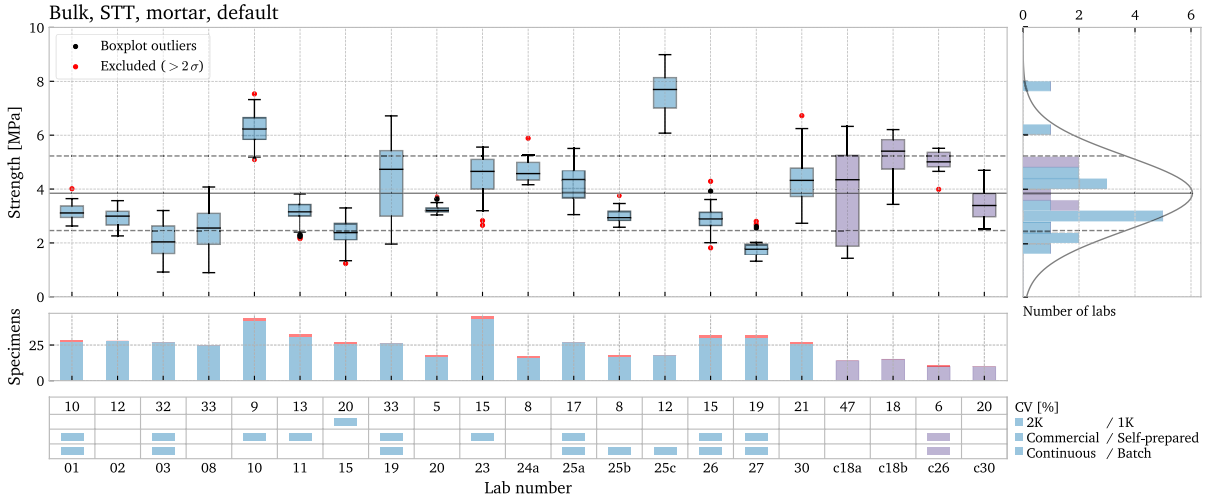

Fig. 27 Splitting tensile strength values obtained by splitting tests performed on specimens of 'mortar' scale, for the 'bulk' orientation (combination of cast specimens and printed specimens loaded in V/W and U/V (cubic, blue) or V.U/W and U.W/V (cylindrical, purple) orientation

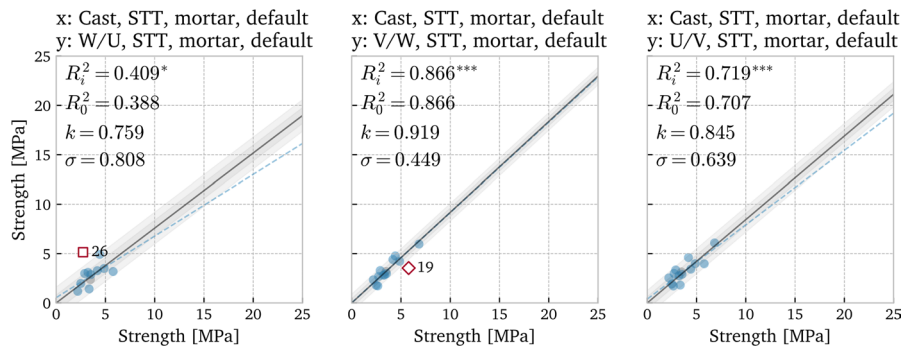

Fig. 28 Correlation between splitting tensile test results for cast specimens and printed specimens loaded in W/U & W.U/V, V/W & V.U/W, and U/V & U.W/V orientation, 'mortar' scale

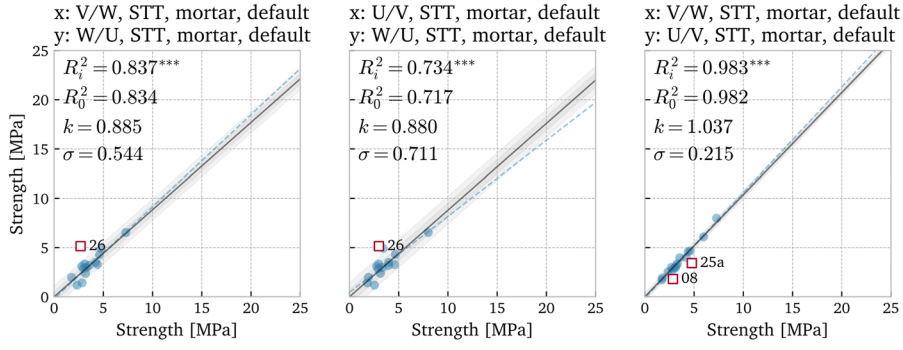

Fig. 29 Correlation between splitting tensile test results for printed specimens loaded in W/U & W.U/V, V/W & V.U/W, and U/V & U.W/V orientation, 'mortar' scale

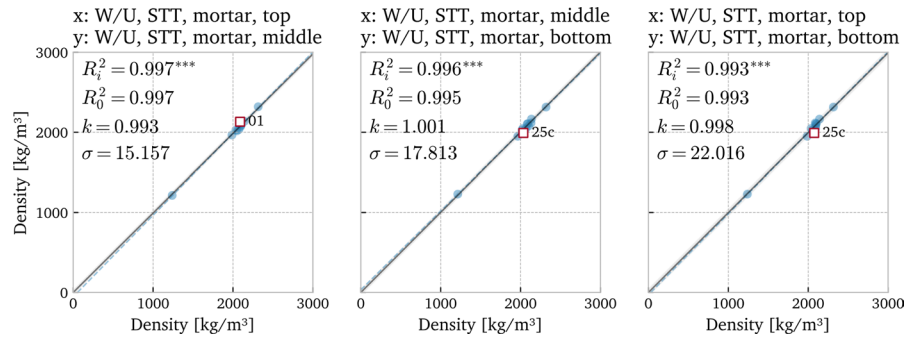

Fig. 30 Correlation between density values for printed specimens loaded in W/U & W.U/V orientation, 'mortar' scale, subtracted from bottom, middle and top locations

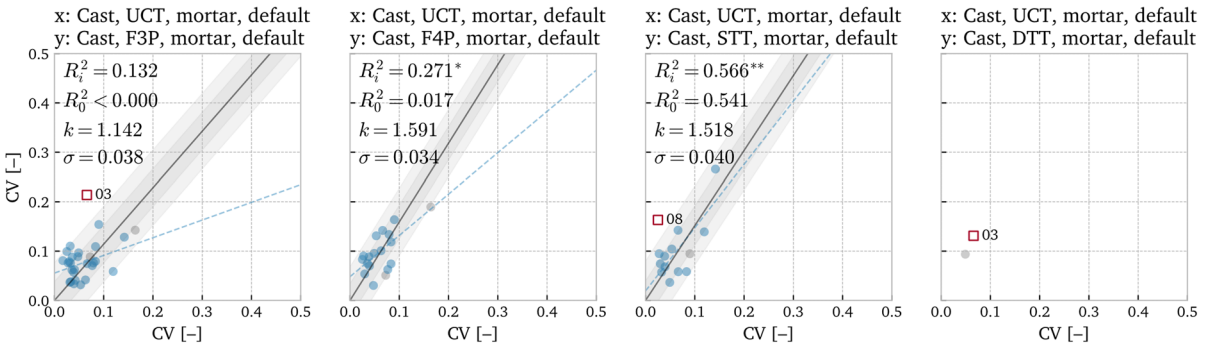

Fig. 31 Correlation plots for coefficient of variation for compression tests and 3-Point bending, 4-Point bending, splitting tensile, and uniaxial tensile tests, performed on cast specimens of 'mortar' scale

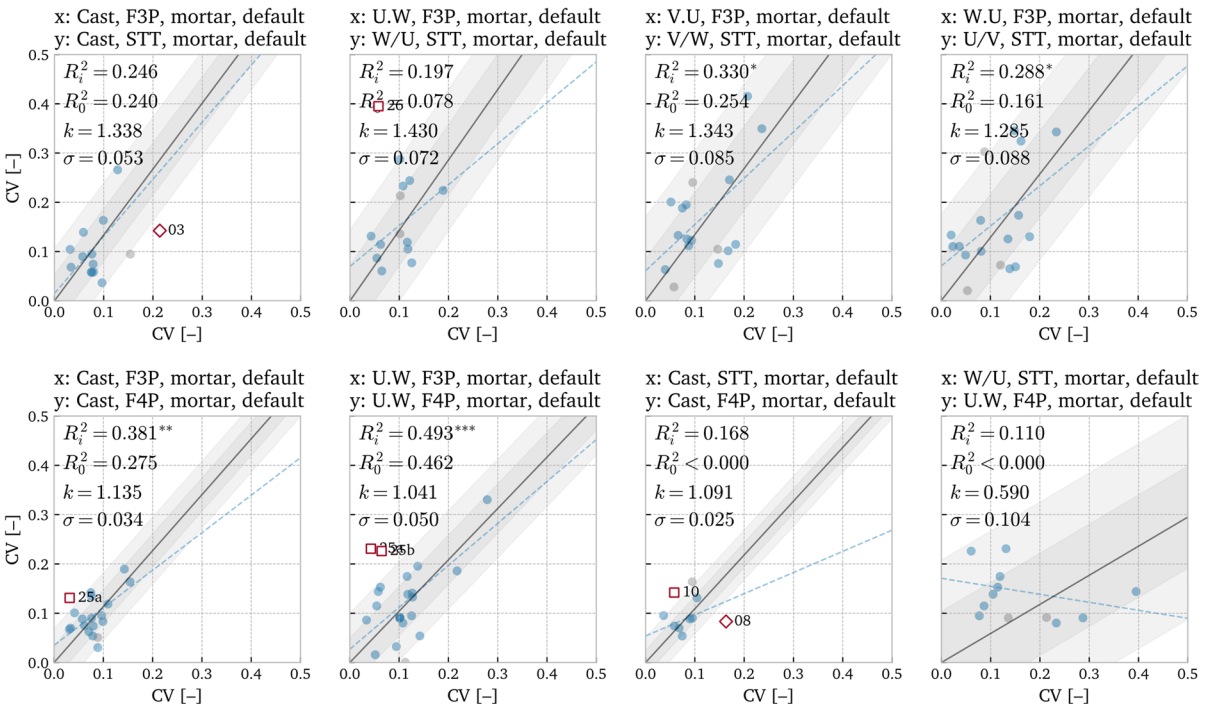

Fig. 32 Correlation plots for coefficient of variation between 3-Point bending, 4-Point bending, splitting tensile, and uniaxial tensile tests, performed on cast and printed specimens of 'mortar' scale

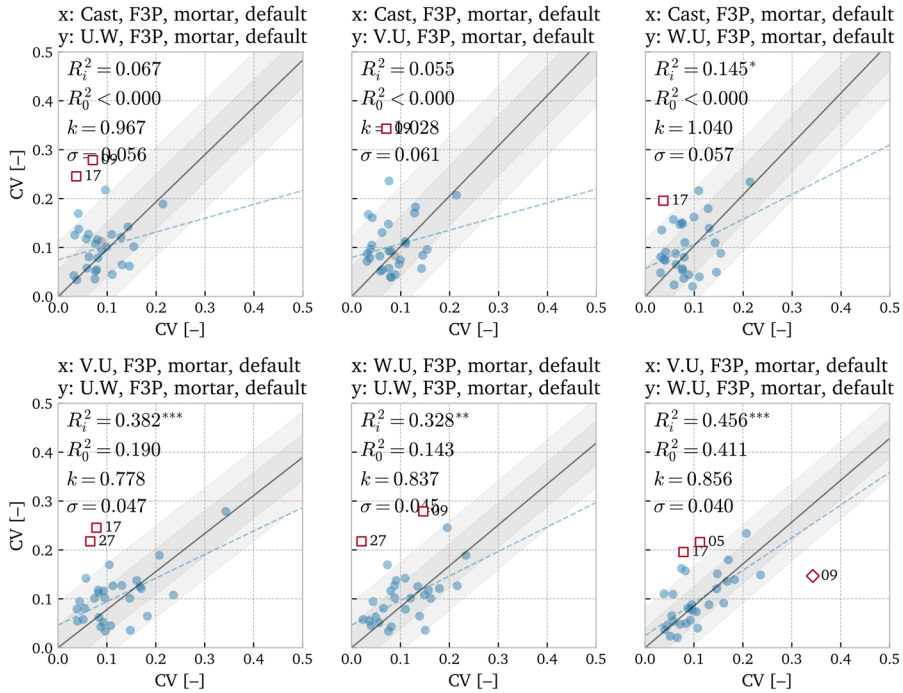

Fig. 33 Correlation plots for coefficient of variation of 3-point bending test results for cast specimens and printed specimens loaded in U.W, V.U, and W.U orientation, 'mortar' scale

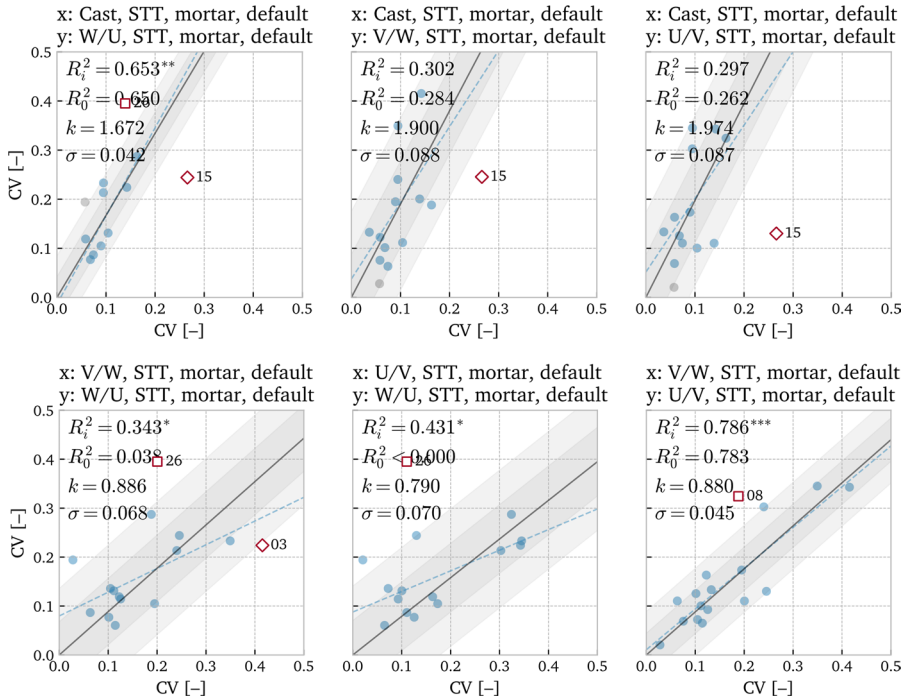

Fig. 34 Correlation plots for coefficient of variation of splitting tensile test results for cast specimens and printed specimens loaded in W/U & W.U/V, V/W & V.U/W, and U/V & U.W/V orientation, 'mortar' scale

Table 7 Parameters of individual labs with outliers in box plots (sec. 3)

Lab ID	✓ Batch / Continuous	✓ 1 K / 2 K	Max grain size	Avg. cast comp. strength [MPa]	Transport length [m]	Nozzle travel speed [mm/s]	Nozzle shape	Outliers in
9	✓	✓	2	80.1	5	×	round	Cast, F3P,F4P
10	✓	✓	4	72.6	20	×	rectangular	V/W,U/V,STT
11	✓	✓	2	37.8	0	116	round	V.U,F3P
16	✓	✓	4	96	10	×	×	V.U,W.U,F3P
23	✓	✓	2	67.7	25	79	round	V.U,F3P, Cast,W/U,STT
24	✓	✓	2	88.1	15	200	round	U/V,STT
25a		✓	2	40.3	15.5	250	rectangular	U/V,STT
25b		✓	×	×	0	80	×	W/U,STT
26		✓	2	49	10	80	round	Cast,U/V,STT
29	✓	✓	0.9	41.2	0	20	round	Cast,F3P,F4P,U.W,F4P

Table 8 Parameters of individual labs with outliers in correlation plots (sec. 4)

Lab	✓ Batch / Continuous	✓ 1 K / 2 K	Max grain size	Avg. cast comp. strength [MPa]	Transport length [m]	Nozzle travel speed [mm/s]	Nozzle shape	Nozzle area [mm^2]	Outlier (number of times)
3		✓	1	51.6	3	150	round	707	1
8	✓	✓	1.18	59.7	0	×	round	314	3
9	✓	✓	2	80.1	5	×	round	491	4
10	✓	✓	4	72.6	20	×	rectangular	2100	1
15	✓		4	42.3	10	300	×	×	1
16	✓	✓	4	96.0	10	×	×	×	3
17	✓	✓	2	52.9	0	10	round	962	3
19		✓	1.2	120.2	15	×	round	1257	10
22	✓	✓	1	96.6	15	45	round	491	1
25a		✓	2	40.3	15.5	250	rectangular	500	4
26		✓	2	49	10	80	round	804	2
27		✓	0.5	48.4	10	41.8	round	804	4

References

1. Bos F, Wolfs R, Ahmed Z, Salet T (2016) Additive manufacturing of concrete in construction: potentials and challenges of 3D concrete printing. Virtual Phys Prototyp 11:209–225. https://doi.org/10.1080/17452759.2016.1209867
2. Xiao J, Ji G, Zhang Y et al (2021) Large-scale 3D printing concrete technology: current status and future opportunities. Cement Concr Compos 122:104115. https://doi.org/10.1016/j.cemconcomp.2021.104115
3. Ma G, Buswell R, Leal Da Silva WR et al (2022) Technology readiness: a global snapshot of 3D concrete printing and the frontiers for development. Cem Concr Res 156:106774. https://doi.org/10.1016/j.cemconres.2022.106774
4. Menna C, Mata-Falcón J, Bos FP et al (2020) Opportunities and challenges for structural engineering of digitally fabricated concrete. Cem Concr Res 133:106079. https://doi.org/10.1016/j.cemconres.2020.106079
5. Bos FP, Menna C, Pradena M et al (2022) The realities of additively manufactured concrete structures in practice. Cem Concr Res 156:106746. https://doi.org/10.1016/j.cemconres.2022.106746
6. Flatt RJ, Wangler T (2022) On sustainability and digital fabrication with concrete. Cem Concr Res 158:106837. https://doi.org/10.1016/j.cemconres.2022.106837
7. Bhattacherjee S, Basavaraj AS, Rahul AV et al (2021) Sustainable materials for 3D concrete printing. Cem Concr Compos 122:104156. https://doi.org/10.1016/j.cemconcomp.2021.104156
8. Mohan MK, Rahul AV, De Schutter G, Van Tittelboom K (2021) Extrusion-based concrete 3D printing from a material perspective: a state-of-the-art review. Cem Concr

Compos 115:103855. https://doi.org/10.1016/j.cemconcomp.2020.103855
9. Bos F, Wolfs R, Ahmed Z, Salet T (2019) Large scale testing of digitally fabricated concrete (DFC) Elements. In: Wangler T, Flatt RJ (eds) First RILEM international conference on concrete and digital fabrication—digital concrete 2018. Springer International Publishing, Cham, pp 129–147. https://doi.org/10.1007/978-3-319-99519-9_12
10. Ahmed Z, Wolfs R, Bos F, Salet T (2022) A framework for large-scale structural applications of 3D printed concrete: the case of a 29 m bridge in the Netherlands. Open Conf Proc 1:5–19. https://doi.org/10.52825/ocp.v1i.74
11. Wolfs R, Bos D, Salet T (2023) Lessons learned of project Milestone: the first 3D printed concrete house in the Netherlands. Mater Today Proc. https://doi.org/10.1016/j.matpr.2023.06.183
12. Bos F, Mechtcherine V, Roussel N, et al. (2023) RILEM TC 304-ADC ILS-mech Study Plan Published on MediaTUM. https://doi.org/10.14459/2023mp1705940
13. Bos F, Menna C, Robens-Radermacher A, et al (2024) Mechanical properties of 3D printed concrete: a RILEM TC 304-ADC interlaboratory study—approach and main results. Manuscript submitted to this Materials & Structures Topical Issue. https://doi.org/10.1617/s11527-025-02686-x
14. Bos F, Robens-Radermacher A, Muthukrishnan S, et al (2024) Database of the RILEM TC 304-ADC interlaboratory study on mechanical properties of 3D printed concrete (ILS-mech). https://doi.org/10.5281/zenodo.12200570. Embargoed until 1 July 2025
15. Robens-Radermacher A, Kujath C, Bos F, Mechtcherine V, Unger JF (2025) Mechanical properties of 3D printed concrete: a RILEM TC 304-ADC Interlaboratory Study – Design and Implementation of a Database System for Querying, Sharing, and Analyzing Experimental Data. Manuscript accepted for this Materials & Structures Topical Issue. https://doi.org/10.1617/s11527-025-02650-9
16. Mechtcherine V, Muthukrishnan S, Robens-Radermacher A, et al (2025) Mechanical Properties of 3D Printed Concrete: a RILEM 304-ADC Interlaboratory Study – Compressive Strength and Modulus of Elasticity. Manuscript accepted for this Materials & Structures Topical Issue. https://doi.org/10.1617/s11527-025-02688-9
17. Le TT, Austin SA, Lim S et al (2012) Hardened properties of high-performance printing concrete. Cem Concr Res 42:558–566. https://doi.org/10.1016/j.cemconres.2011.12.003
18. Wolfs RJM, Bos FP, Salet TAM (2019) Hardened properties of 3D printed concrete: the influence of process parameters on interlayer adhesion. Cem Concr Res 119:132–140. https://doi.org/10.1016/j.cemconres.2019.02.017
19. Kruger J, Van Zijl G (2021) A compendious review on lack-of-fusion in digital concrete fabrication. Addit Manuf 37:101654. https://doi.org/10.1016/j.addma.2020.101654
20. Mechtcherine V, Van Tittelboom K, Kazemian A et al (2022) A roadmap for quality control of hardening and hardened printed concrete. Cem Concr Res 157:106800. https://doi.org/10.1016/j.cemconres.2022.106800
21. Neville AM (2011) Properties of concrete, 5th edn. Pearson, Harlow Munich
22. Oluokun F (1991) Prediction of concrete tensile strength from its compressive strength: an evaluation of existing relations for normal weight concrete. ACI Mater J. https://doi.org/10.14359/1942
23. O'Cleary DP, Byrne JG (1960) Testing concrete and mortar in tension. Engineering 18:384–385
24. Walker S, Bloem DL (1957) Studies of flexural strength of concrete—part 3: effects of variations in testing procedures. Proc ASTM 57:1122–1139